Research Square

Preprints are preliminary reports that have not undergone peer review.
They should not be considered conclusive, used to inform clinical practice,
or referenced by the media as validated information.

Lead Removal using Natural Clay vs. Recycled Concrete Debris: Adsorption Performance and Life Cycle Assessment (LCA)

Radia Maachou
University of Sciences and Technology Houari Boumediene
Hiba Ferhat
University of Sciences and Technology Houari Boumediene
Abdelouahab Lefkir
Ecole Nationale Supérieure des Travaux Publics
Hakim Baloul
University of Boumerdes
Abdelghani Bouchama
Université de Mostaganem
Yazid Chetbani
Centre de Recherche Scientifique et Technique en Analyses Physico-Chimiques
Mostefa Hani
University of Jijel
Nadjib Mebirouk
University of Skikda
Ahmed Belaadi
University of Skikda
Herbert Mukalazi
hmukalazi@kyu.ac.ug

Kyambogo University

Article

Keywords: Adsorption, Life Cycle Assessment (LCA), Greenhouse gas emissions, Recycled concrete, Natural clay, Lead removal

Posted Date: November 25th, 2026

DOI: https://doi.org/10.21203/rs.3.rs-11703931/v1

License: This work is licensed under a Creative Commons Attribution 4.0 International License.
Read Full License

Additional Declarations: No competing interests reported.

Lead Removal using Natural Clay vs. Recycled Concrete Debris: Adsorption Performance and Life Cycle Assessment (LCA)

Radia Maachou[1], Hiba Ferhat[1], Abdelouahab Lefkir[2], Hakim Baloul[3], Abdelghani Bouchama[4,5], Yazid Chetbani[5], Mostefa Hani[6], Nadjib Mebirouk[7], Ahmed Belaadi[8,*], and Herbert Mukalazi[9,*]

1. Laboratoire d'Électrochimie-Corrosion, Métallurgie et Chimie Minérale (LECMCM), Université des Sciences et de la Technologie Houari Boumediene (USTHB), Alger, Algérie.
2. LTPiTE Laboratory. École Nationale Supérieure des Travaux Publics (ENSTP), Algiers, Algeria.
3. Food Technology Research Laboratory (LRTA), Faculty of Sciences Engineer, M'hamed Bougara University.
4. Technical Platform for Physical and Chemical Analysis (PTAPC) Mostaganem, University of Mostaganem, Algeria.
5. Centre de Recherche scientifique et Technique en Analyses Physico-Chimiques CRAPC, BP 384, Bou-Ismail, RP 42004, Tipaza, Algeria.
6. Department of Civil Engineering and Hydraulics, Faculty of Sciences and Technology, University of Jijel,18000 Jijel, Algeria.
7. LMGHU Laboratory, Department of Civil Engineering, University 20 Aout 1955 Skikda, Algeria.
8. Department of Mechanical Engineering, Faculty of Technology, University 20 Août 1955-Skikda, ElHadaiek Skikda, Algeria.
9. Department of Mathematics and Statistics, Kyambogo University, Kampala, Uganda.

*Correspondences: A. Belaadi: ahmedbelaadi1@gmail.com; H. Mukalazi: hmukalazi@kyu.ac.ug

Highlights

- Recycled Concrete Debris (RCD) demonstrates superior efficacy compared to clay in the removal of lead (Pb^{2+}) from aqueous solutions.
- RCD demonstrates complete removal of Pb^{2+} at a dosage of clay that is less than 50% of the amount typically required.
- The maximum adsorption capacity of RCD is 12.13 mg/g, which exceeds that of clay by more than a factor of two.
- Inherent alkalinity effectively treats effluent without the need for pH-adjusting reagents.
- LCA demonstrates that RCD significantly mitigates impacts related to climate, toxicity, and resource utilization.

Abstract

Life Cycle Assessment (LCA) is a comprehensive approach for assessing the environmental effects of a process throughout its full life span, encompassing resource extraction through to waste disposal. By facilitating comparisons between various technologies, LCA aids in creating more sustainable and environmentally responsible solutions. In this study, LCA was applied to assess the environmental performance of two adsorbent materials: Recycled Concrete Debris (RCD) and natural clay sourced from the Mostaganem site. The analysis encompassed all stages of their life cycle, including extraction or recycling, utilization, and end-of-life management. The study first compared the effectiveness of the two materials in removing lead ions (Pb^{2+}) from contaminated water. Some parameters, such as the effect of mass, metal concentration, effect of pH, and contact time, were studied to compare the elimination of the Pb^{+2} by both of the materials. In the second part, LCA was employed to evaluate and contrast their environmental impacts. Environmental impacts of the different stages of the process, from the collection and preparation of the scrap to the management of the metal-saturated residues. The results demonstrate that RCD outperforms natural clay in lead removal, achieving elimination rates of 100% and 98%, respectively. Furthermore, recycled debris exhibits significant environmental advantages, including lower greenhouse gas emissions, reduced energy consumption, and enhanced cost-efficiency. These findings highlight RCD as a sustainable and economically viable alternative for treating lead-contaminated water.

Keywords: Adsorption; Life Cycle Assessment (LCA); Greenhouse gas emissions; Recycled concrete; Natural clay; Lead removal.

Graphical abstract:

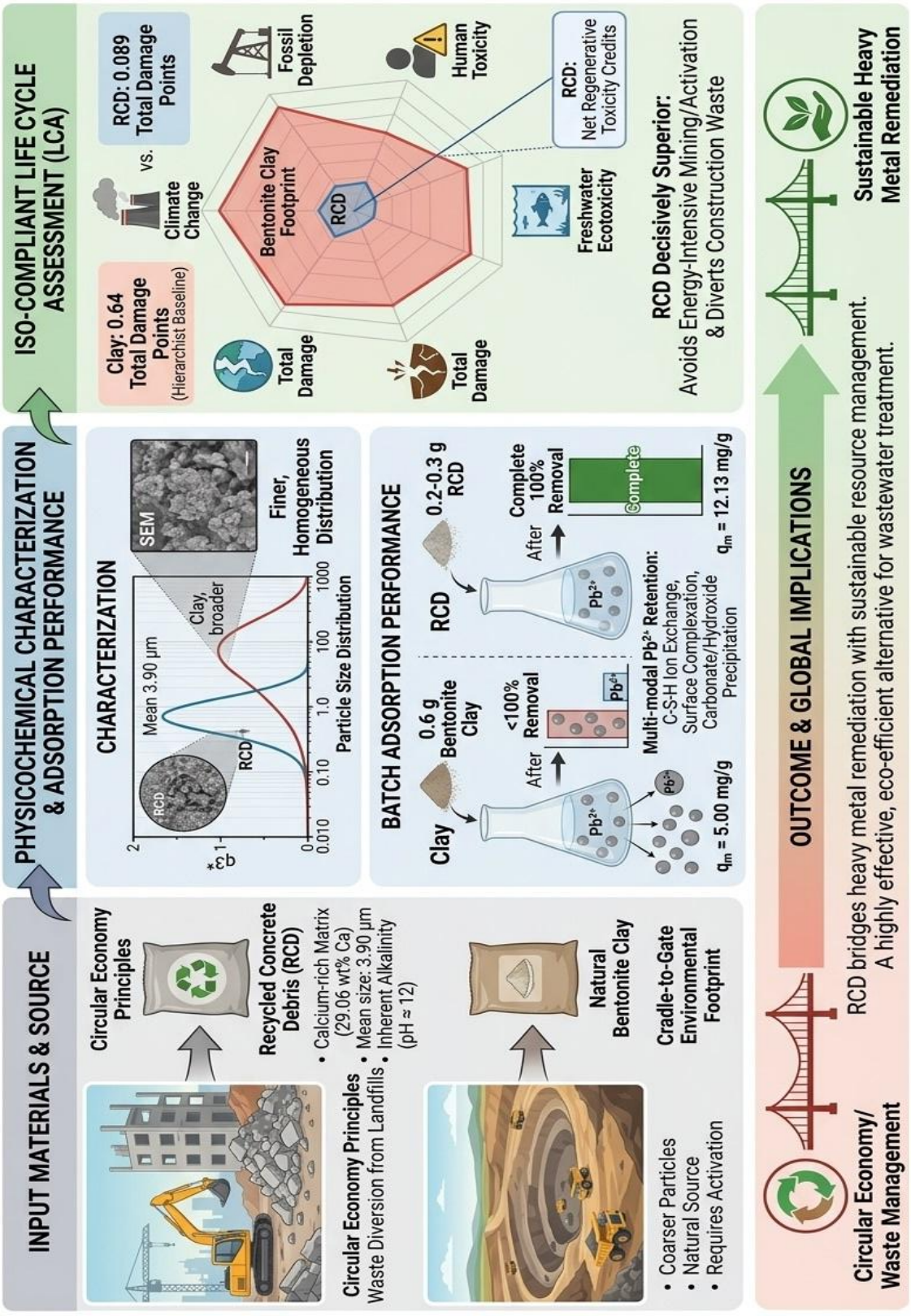

1 Introduction

In recent decades of urbanization, numerous obsolete buildings have been demolished, resulting in the generation of billions of tons of construction waste. As of 2018, China accumulated over 20 billion tons

of construction waste, a situation that is also occurring in numerous other countries globally [1], [2], [3], [4], [5], [6]. Water pollution has become a major global issue, primarily caused by the increased use of heavy metals in industrial processes and the discharge of untreated effluents [7], [8] . This issue is exacerbated by population growth, rapid urbanization, and industrial expansion [9], [10]. Among these pollutants, lead is of particular concern due to its high toxicity, persistence, and tendency to bioaccumulate in aquatic ecosystems, posing a severe risk to human health and the environment [11]. To address this threat, adsorption has emerged as one of the most attractive and effective treatment methods, owing to its operational simplicity, flexibility, and moderate cost [12], [13], [14].

In this context, natural or modified clays have been extensively studied due to their high specific surface area, elevated cation exchange capacity, and widespread availability [9], [14]. However, the extraction of these materials causes environmental disturbances to natural deposits, and their processing frequently requires energy-intensive chemical or thermal activations, thereby limiting their overall ecological sustainability [15]. To mitigate these impacts, the valorization of industrial by-products and construction and demolition waste (CDW) constitute an innovative and eco-friendly alternative [15]. Globally, annual solid waste generation exceeds 2.01 billion tons [16], with the building sector contributing 30 to 40%. More specifically, annual CDW generation is estimated at nearly 3 billion tons, 40 to 60% of which consists of concrete debris [17].

Due to the carbon footprint associated with its manufacturing and the difficulty of separating its original components, end-of-life concrete represents a significant environmental burden. Its physical processing through crushing, screening, and grinding into a fine powder thus offers a valorization opportunity as a low-cost adsorbent [17], [18], helping to alleviate pressure on landfills while aligning fully with the circular economy model. On a local scale, Algeria is fully confronted with this challenge. Accelerating urbanization and infrastructure modernization generate massive volumes of residue, increasing pressure on overall waste management. While models by Hoornweg and Bhada-Tata [19] had already projected a steady increase in national solid waste production, rising from 23,288 tons per day (1.21 kg/capita/day) to nearly 46,078 daily tons (1.45 kg/capita/day) by 2025 [20], the fraction generated by the construction and civil engineering sector remains very poorly valorized. The progressive saturation of national technical landfill centers (CET) thus makes the development of local recycling channels for this mineral debris crucial. However, the majority of academic studies dedicated to heavy metal adsorption remain limited to evaluating laboratory-scale physicochemical performance (retention capacities, kinetics, and isotherms), overlooking the overall environmental impacts associated with the extraction, preparation, or transport of adsorbent matrices. Evaluating a material solely through its efficiency in aqueous solution provides only a partial view of its ecological viability.

Life Cycle Assessment (LCA) thus stands out as a rigorous decision-making tool to quantify environmental footprints from "cradle-to-gate". In this perspective, applying LCA allows for comparing

the ecological sustainability of natural clay to that of Recycled Concrete Debris (RCD) for lead removal by coupling experimental adsorption parameters with a comprehensive carbon and energy balance.

Similarly, recent studies have examined the mechanical, thermal, microstructural, and flexural strengths, as well as the mechanical properties of concrete, in connection with similar behaviors observed in other materials. They have analyzed the influence of these mechanical properties on pykrete, sisal-fiber-reinforced foamed concrete, compressed earth blocks, granular soils, self-compacting and sprayed concretes, recycled aggregate, hydrated plaster, hemp fibers, brick waste powder, and high-performance fiber-reinforced concrete [21], [22], [23], [24], [25], [26], [27]. Salah and Hani [28] conducted an investigation into the impact of elevated temperatures on the compressive strength of self-compacting concrete. Utilizing recycled materials such as gravel results in a reduction of the amount of gravel that must be extracted from the earth. Furthermore, they serve as a foundation for road construction, minimizing the environmental impact of material transportation and decreasing related costs [6].

The main objective of this study is to perform an integrated comparative evaluation between natural clay (from the Mostaganem deposit) and RCD (from a technical landfill center) for lead retention in aqueous media. Adsorption experiments were conducted in a batch system under mechanical agitation to determine the influence of key operational factors (pH, contact time, adsorbent dose, and initial concentration) as well as the mechanisms governing the process (kinetics and isotherms). Concurrently, a comparative LCA focusing on the carbon footprint and energy consumption was carried out to assess the overall impact of each pathway, from material acquisition to implementation. Finally, this paper details the characterization of the adsorbents, presents the experimental and environmental results, and discusses the optimal trade-off between treatment efficiency and sustainability.

2 Materials and methods

2.1 Material preparation and Provenance

The clay used in this study is extracted from the M'Zila quarries in the Mostaganem province, a major Algerian industrial clay deposit (**Figure 1**) and transported to the National Company of Non-Ferrous Mining Products and Useful Substances (Entreprise Nationale des Produits Miniers Non Ferreux et des Substances Utiles (ENOF) located in Elharach (Algiers). At this facility, the raw clay undergoes a multi-step preparation process consisting of: (i) storage and chemical activation using magnesium oxide (MgO) and soda ash (Na_2CO_3); (ii) crushing and thermal drying; (iii) grinding coupled with dust removal to achieve a particle size suitable for wastewater treatment applications; and (iv) final bagging prior to transportation to the treatment site.

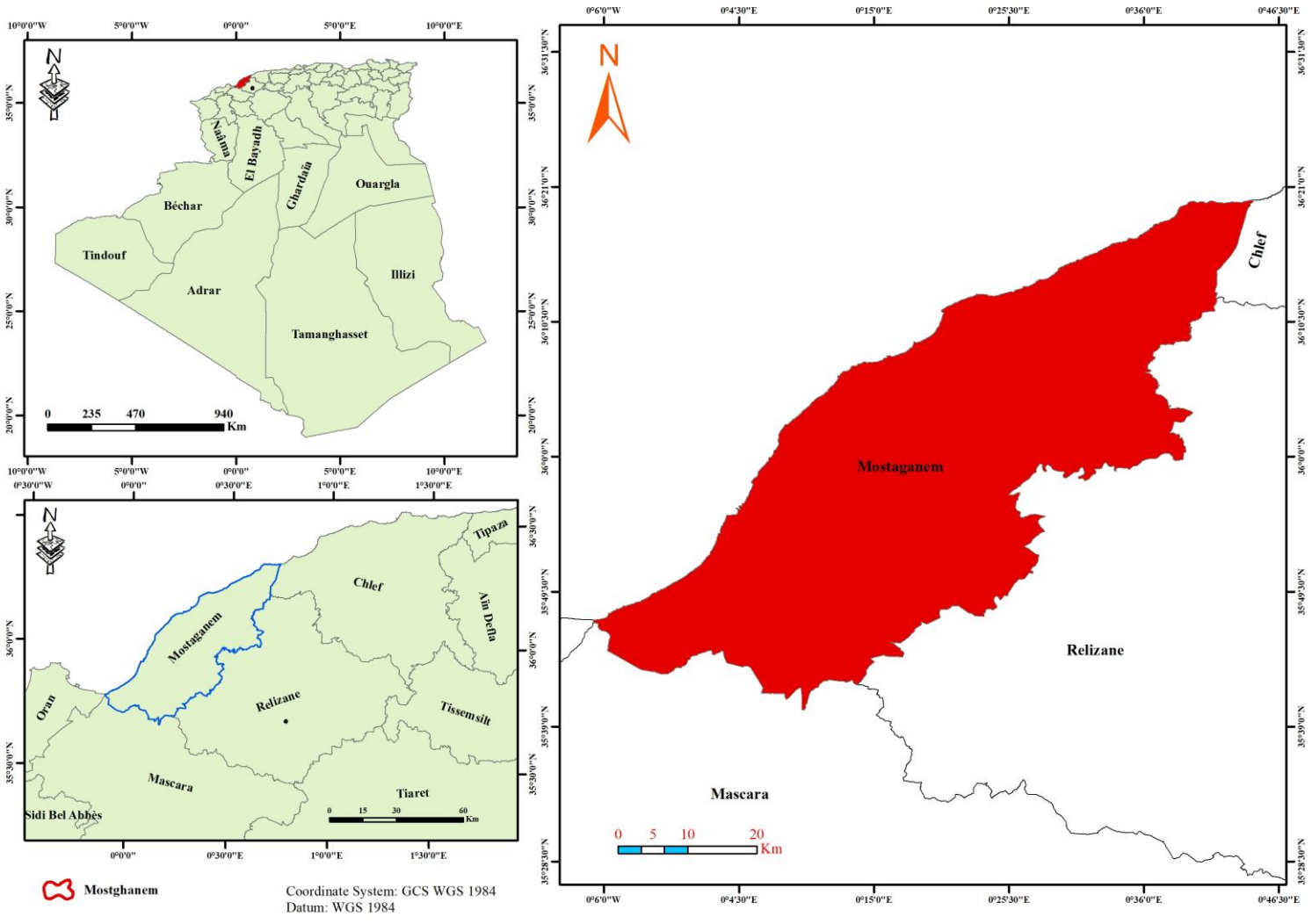

Figure 1. Geographic view of the M'Zila deposit.

At the same time, construction waste is collected at the Hamici landfill located in the municipality of Mahelma, approximately 30 km southwest of Algiers (**Figure 2**). This construction waste, consisting mainly of concrete, is also crushed and screened on site to achieve an optimum particle size, so that it can be used as an adsorbent to remove heavy metals from wastewater.

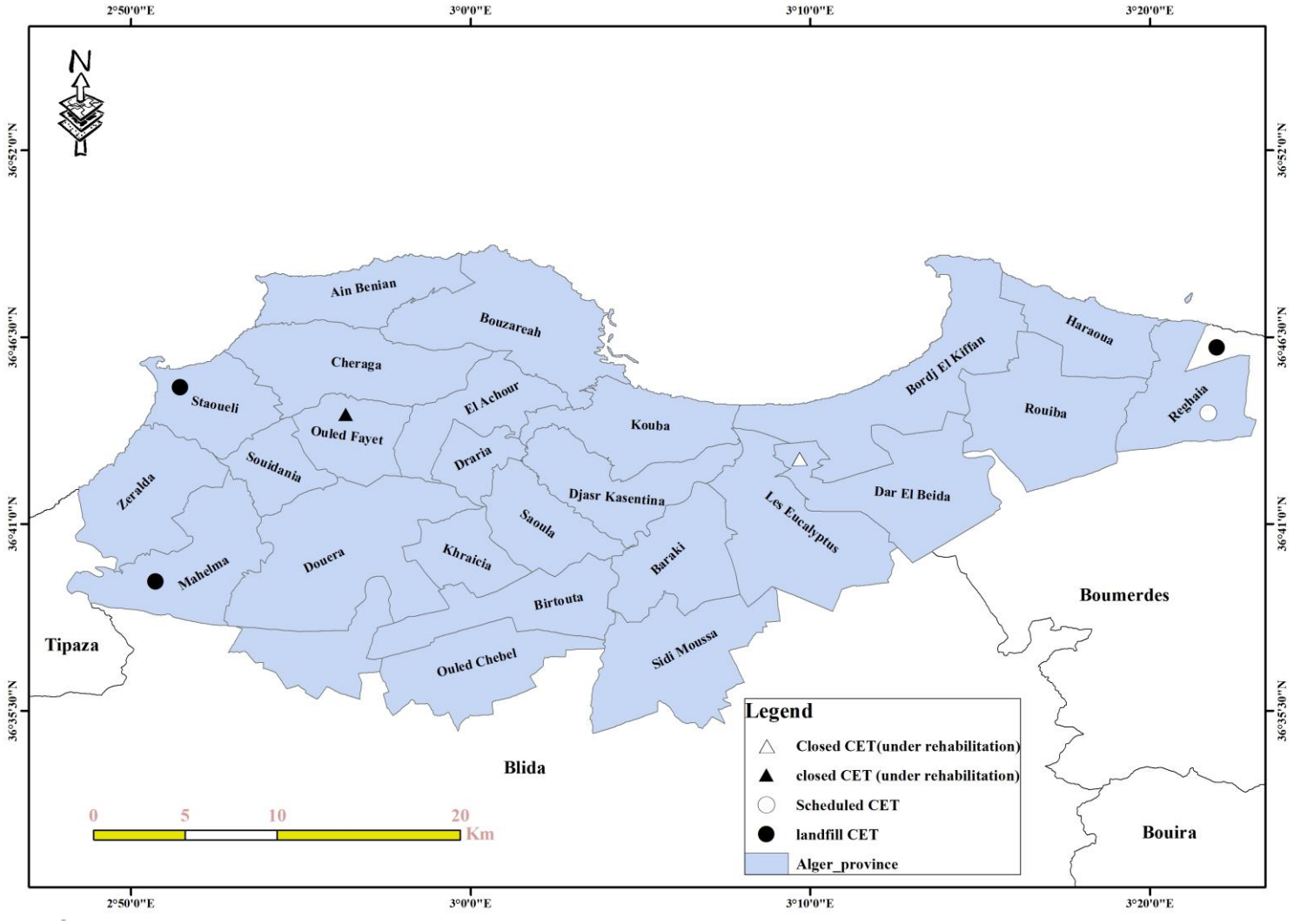

Figure 2. Geographical distribution of technical landfill centers (CET) in the Wilaya of Algiers.

This specific preparation of the two materials, clay and debris, aims to maximize their effectiveness as adsorbents, while respecting the technical and environmental constraints associated with their use.

2.2 Adsorbent characterization

2.2.1 Morphological and Elemental Characterization (SEM/EDX)

The surface morphology and localized elemental composition of the natural clay and recycled debris were examined using a ThermoFisher Phenom scanning electron microscope. The instrument was equipped with an energy-dispersive X-ray (EDX) detector and operated using the Phenom User Interface software (version 1.9.17). Representative microscopic images and corresponding EDX spectra were acquired for each sample to observe their structural features and map the distribution of specific elements on the material surfaces.

2.2.2 Thermogravimetric Analysis (TGA)

The thermal stability and decomposition behavior of the natural clay and recycled debris were evaluated using thermogravimetric analysis (TGA). The tests were performed with a Setaram Setsys 16/18 thermobalance. The samples were heated at a controlled rate under a specific gas atmosphere, and their mass changes were recorded continuously as the temperature increased. This allowed for the precise observation of thermal degradation and compositional changes within the materials.

2.2.3 Laser Particle Size Analysis

The particle size distribution of the materials was measured using a Horiba LA-960A laser diffraction analyzer. The analysis was performed in liquid mode with distilled water as the dispersing medium.

2.3 Batch adsorption experiments

Adsorption experiments were carried out in 50 mL Erlenmeyer flasks using Recycled Concrete Debris (RCD) and bentonite clay. Both RCD and natural clay were utilized in their natural, untreated state, requiring no thermal or chemical activation. Batch adsorption experiments were carried out at ambient temperature (18–20 °C) with constant mechanical agitation at 400 rpm. As a result, the energy demand for the preparation phase is negligible, since the process relies solely on raw, locally available materials and standard mechanical mixing.

The pH was monitored by immersing an electrode directly into the solution. Each experiment lasted 60 minutes. After this time, the mixtures were centrifuged, and the remaining concentrations of Pb^{2+} was measured using atomic absorption spectroscopy. The influence of several factors: adsorbent mass, pH, initial metal concentration, and contact time were studied by changing one variable at a time while keeping all other conditions constant. **Figure 3** shows the experimental setup used.



Figure 3. Experimental setup of adsorption process.

The masses tested varied from 0.1 to 2 g. Then pH-dependent experiments followed, ranging from 2 to 12 using HCl or NaOH (0.1– 4 M). Once optimal pH conditions were established (pH of 5.5 for Pb^{2+}), metal-ion concentrations were varied between 10 and 100 ppm. Finally, contact time was varied from 5 to 60 minutes to evaluate adsorption kinetics for both adsorbents. The adsorption efficiency of the pollutant (η) was calculated using **Equation (1)**:

$$\eta = \frac{C_i - C_e}{C_i} \times 100 \quad (1)$$

Where C_i and C_e (mg/g) represents initial and the equilibrium concentrations of the metal ions in solution.

2.4 Hydrodynamic Scale-Up and Reactor Similitude

To transpose the experimental performance of lead (Pb^{2+}) adsorption onto raw clay and RCD from laboratory batch tests to a prototype scale (1 m^3), a rigorous hydrodynamic scale-up approach based on reactor similitude was established.

2.4.1 Geometric Similitude and Scale Factor

Figure 4 presents the simplified scale-up geometry and speed comparison. The laboratory-scale batch tests were conducted in cylindrical reactors with an active liquid volume $V_M = 50$ mL (5×10^{-5} m^3), a vessel diameter $T_M = 10$ cm, and an agitation speed $N_M = 400$ rpm. Geometric similarity between the model (index M) and the prototype (index P) was maintained by preserving constant geometric ratios ($H/T =$ const., $D/T =$ const., where H is the liquid height, T is the vessel diameter, and D is the impeller diameter). The volumetric scale-up factor R_V and the linear geometric scale ratio λ are defined as **Equation (2)**:

$$\lambda = \left(\frac{V_P}{V_M}\right)^{1/3} = (20\,000)^{1/3} \approx 27 \quad (2)$$

Applying this linear scale factor ($\lambda = 27$) yields the geometric dimensions for the prototype reactor: Vessel Diameter $T_P = \lambda \cdot T_M = 270$ (cm) and Liquid Height $H_P = 17.5$ (cm)

2.4.2 Scale-Up Criterion: Constant Volumetric Power Input ($P/V =$ const.)

In solid-liquid heterogeneous systems, maintaining a constant volumetric power dissipation rate ($P/V =$ const.) is widely recognized as the standard industrial scale-up criterion [29]. This criterion ensures equivalent turbulent dissipation rates and liquid-solid mass transfer coefficients (k_s) across scales, preventing mass transfer limitations from altering adsorption kinetics during scale-up.

Under turbulent flow conditions ($Re > 10^4$), the power consumption P of a baffled stirred vessel is expressed as **Equation (3)**:

$$P = N_p \rho N^3 D^5 \quad (3)$$

Where N_p is the dimensionless power number, ρ is the fluid density, N is the rotational agitation speed, and D is the impeller diameter. Assuming geometric similarity and constant fluid density, the volumetric power input ratio simplifies to **Equation (4)**:

$$\frac{P}{V} = \frac{N^3 D^5}{D^3} = N^3 D^2 \tag{4}$$

Setting $(P/V)_P = (P/V)_M$ yields the relationship between the model speed (N_M) and the prototype speed (N_P) as **Equation (5)**:

$$N_P^3 D_P^2 = N_M^3 D_M^2 \Longrightarrow N_P = N_M \cdot \left(\frac{D_M}{D_P}\right)^{2/3} = N_M \cdot \lambda^{-2/3} \tag{5}$$

Substituting $N_M = 400$ rpmand $\lambda = 27$:; $N_P = 400 \times (27)^{-2/3} \approx 44.3$ rpm. **Figure 4** presents the simplified scale-up geometry and speed comparison.

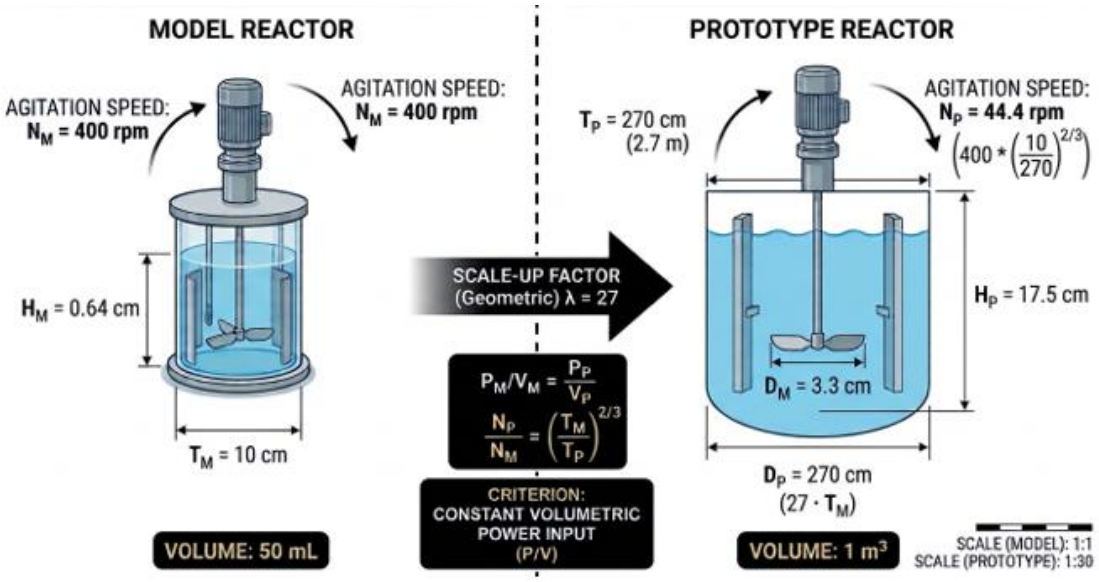

Figure 4. Simplified scale-up geometry and speed comparison.

Extrapolating the mass-to-volume ratio (m/V = const.) to the 1 m^3 functional unit (treatment of 1 $m^3$of effluent containing 50 mg/LPb^{2+}) yields the following inventory input requirements:

Raw Clay: 0.60 g/50 mL $\Longrightarrow$ 12.0 kg/m^3(90% removal $\Longrightarrow$ 45.0 g Pb captured,)

RCD: $\frac{0.20\text{ g}}{50\text{ mL}} \Longrightarrow$ 4 kg/m^3(98% removal $\Longrightarrow$ 49.0 g Pb captured).

The adoption of P/V = const. ensures that the mixing power density is held constant across scales, providing a consistent thermodynamic and kinetic basis for comparative environmental impact assessment within circular economy frameworks [29].

2.5 Life Cycle Assessment (LCA)

LCA is defined as the compilation and evaluation of the outputs and potential environmental impacts of a product system throughout its life cycle [30], [31]. LCA is a rigorous method used to evaluate the environmental impacts associated with all stages of a product's life, from raw material extraction to end-of-life management, including processing, distribution, and use. In this study, LCA is applied to compare the environmental performance of two adsorbent materials, recycled debris and natural clay, in removing lead (Pb^{2+}) from wastewater. This approach addresses the increasing demand for sustainable and eco-friendly water treatment solutions. By examining resource consumption and potential environmental burdens, LCA provides valuable insights for optimizing material use and reducing adverse environmental effects [32], [33] [34] .

This environmental assessment tool quantifies the impacts of a product or process throughout its entire existence, from resource extraction to final disposal [34]. When applied to adsorbents such as clay and recycled debris for heavy metal removal, LCA helps identify the most environmentally significant stages and supports the development of more sustainable water treatment practices. Standard LCA methodology was implemented for the study. The four steps according to ISO standards are: goal and scope definition, life cycle inventory analysis, life cycle impact assessment, and interpretation [32], [35].

2.5.1 Goal and Scope Definition

The objective of this study is to compare the environmental impacts of two batch systems of the adsorption processes for the removal of lead from polluted water in the Algerian context, according to the type of adsorbent material used: (i) bentonite clay and (ii) RCD. This comparison aims to (1) identify the environmentally preferable option, (2) determine the main environmental hotspots within each treatment chain, and (3) quantify the contribution of upstream material preparation to the overall environmental impacts.

2.5.1.1 Functional Unit

The functional unit is defined as the treatment of 1.00 m^3 of water polluted with Pb^{2+}. In accordance with ISO 14044 [36], this functional unit ensures functional equivalence by coupling the water volume with the specific adsorbent masses and removal efficiencies determined experimentally from mass and pH effect evaluations.

2.5.1.2 System Boundaries

The system boundaries define the unit processes included in the LCA. In this comparative study, distinct boundaries were established for each material based on their origin.

For the natural clay, a "cradle-to-grave" approach was adopted (**Figure 5**). The system boundary encompasses eight main operational stages. This includes the extraction of raw bentonite and its initial transport, chemical activation using MgO and Na_2CO_3, intermediate physical treatments (crushing,

drying, grinding, and dust removal), bagging, transportation, and the final lead adsorption process in the laboratory.

Conversely, for the RCD, the system boundary begins directly at the waste processing phase (**Figure 6**). A "zero burden" assumption was applied, meaning the environmental impacts associated with the initial concrete production and building demolition were completely excluded. The system covers five operational stages: crushing and grinding of the collected waste concrete, bagging, transportation, and the final adsorption process.

For both systems, the boundaries conclude with the generation of the adsorption outputs, specifically the treated water and the lead-loaded solid waste.

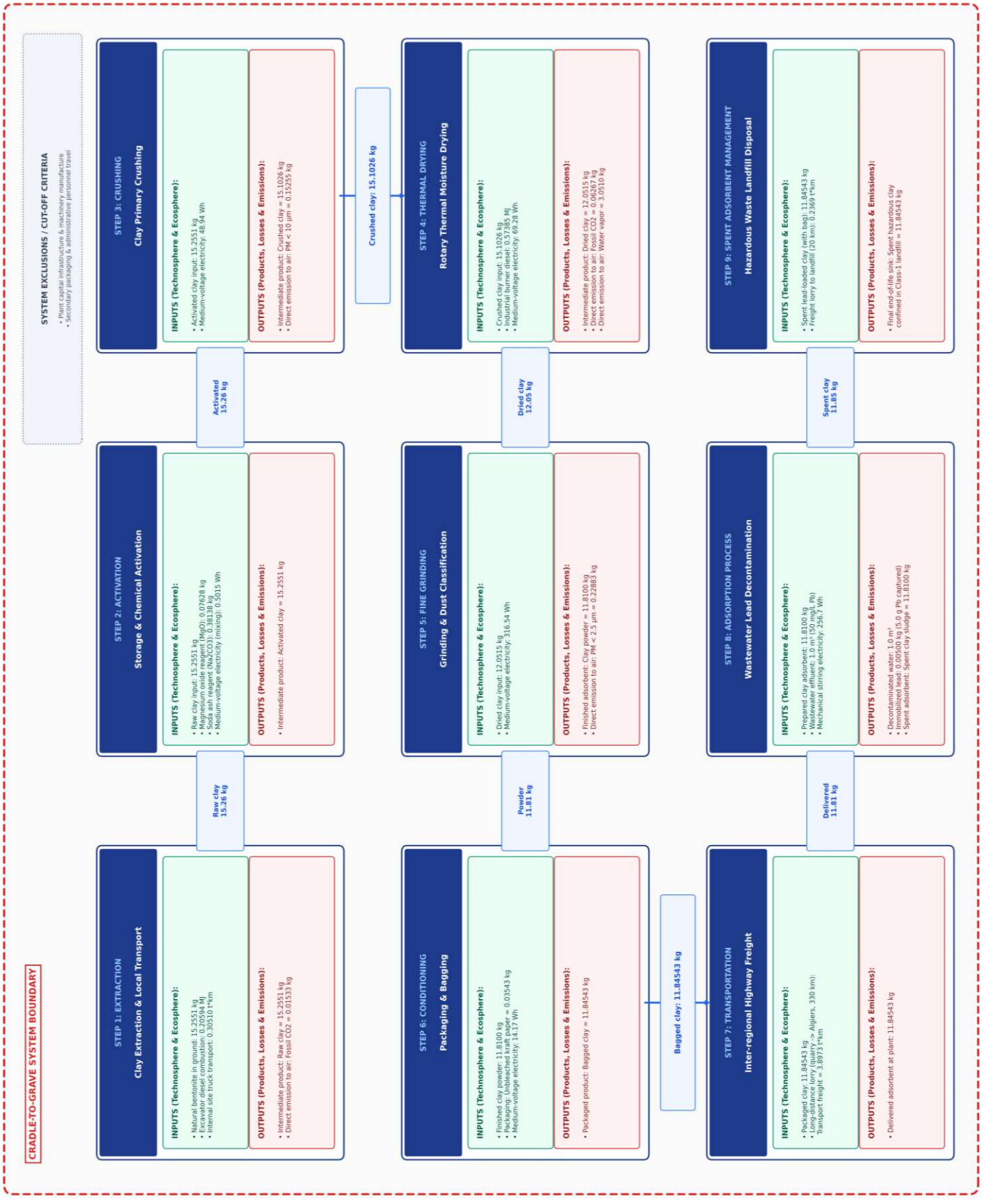

Figure 5: System boundary and process flow diagram of the bentonite clay adsorption system (Cradle-to-Grave).

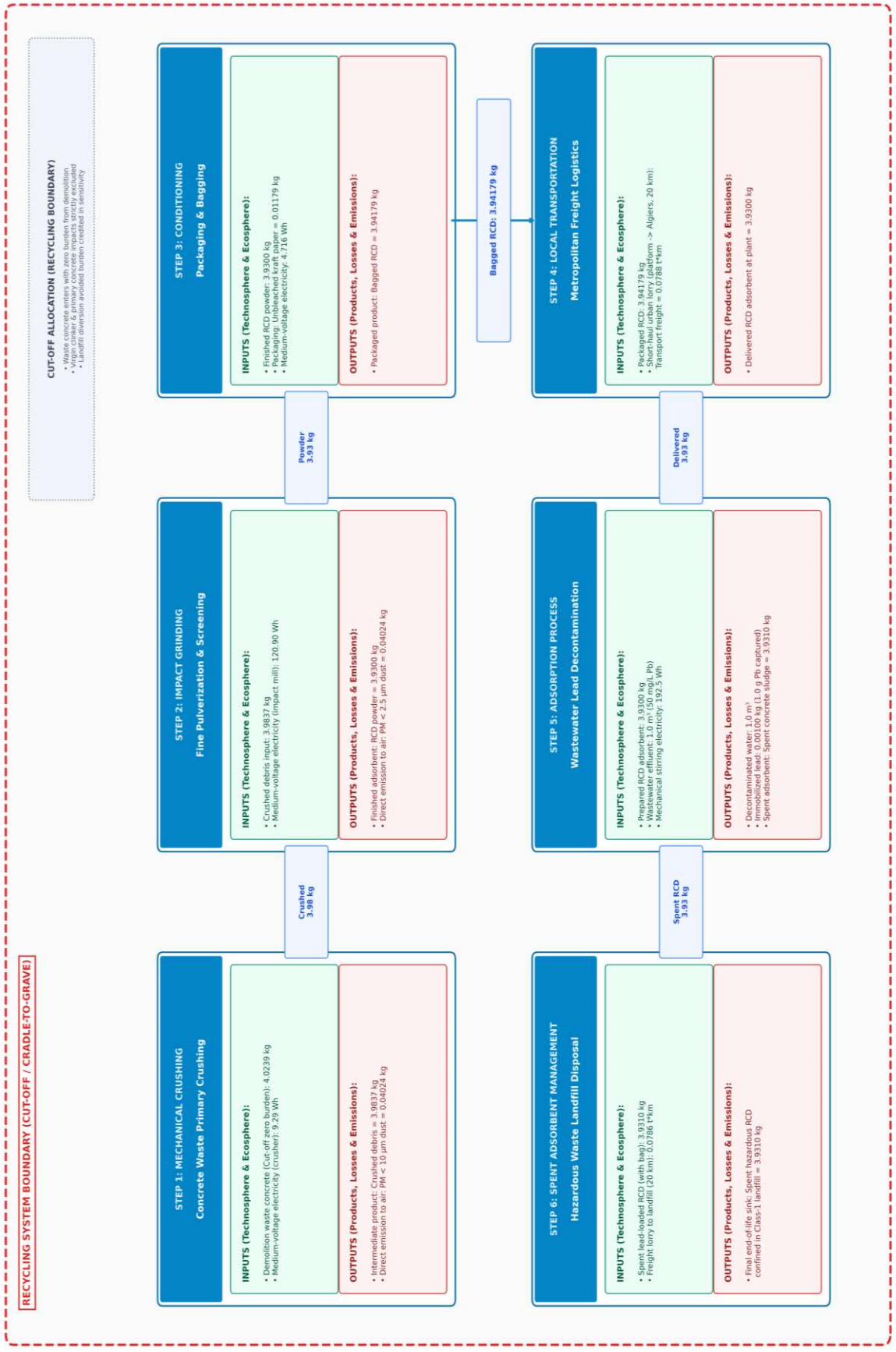

Figure 6: System boundary and process flow diagram of the RCD system.

2.5.2 Life cycle Inventory Analysis

The Life Cycle Inventory (LCI) is a fundamental component of the LCA, designed to systematically identify and categorize the resources consumed (inputs) and the emissions or wastes produced (outputs) across the life cycle of the two adsorbents, natural clay and recycled debris, used for heavy metal removal from wastewater. This inventory compiles data on energy consumption, natural resource use, atmospheric emissions, liquid and solid discharges, and other environmental outputs associated with each stage of the process, from material preparation to adsorption and waste management.

Specifically, the LCI model incorporates the exact experimental mass loads (0.60g/50mL and 0.20g/50mL translate into 11.81kg/m3 and 4 kg/m3 at the industrial batch scale 1.0m3) and their corresponding effluent qualities (residual concentrations of 1 mg/L for RCD and 5 mg/L for clay from an initial 50 mg/L influent, achieving 98% and 90% removal efficiency, respectively). This approach provides a realistic and rigorous basis for environmental comparison while highlighting the superior mass efficiency and direct regulatory compliance of RCD.

The life cycle inventory for the preparation and utilization of both natural clay and RCD is detailed in **Tables 1** and **2**.

For clay (**Table 1**), the process starts with extraction from a natural deposit in Mostaganem. Inputs include the raw clay material and energy for extraction activities, while outputs encompass dust emissions from quarrying. The clay is then transported to the National Non-Ferrous Mining Products Company (ENOF) in Elharach via truck, with inputs such as fuel and outputs including transport-related emissions (e.g., CO_2).

Table 1: Life cycle inventory of clay system.

Process step	Inputs	Quantity (input)	Outputs	Quantity (output)
Clay extraction & transport	Clay bentonite, in ground	15.2551 kg	Raw clay	15.2551 kg
	Diesel burned in building machine	0.20594 Mj	Carbon dioxide, fossil	0.01533 kg
	Transport, freight, lorry	0.30510 t*km		
Storage + chemical activation	Raw clay	15.2551 kg	Activated clay	15.2551 kg
	Magnesium oxide (MgO)	0.07628 kg		
	Soda ash (Na_2CO_3)	0.38138 kg		
	Electricity, medium voltage	0.5015 Wh		
Crushing of clay	Activated clay	15.2551 kg	Crushed clay	15.1026 kg
	Electricity, medium voltage	48.94 wh	Particulates, < 10 µm	0.15255 kg
Drying of clay	Crushed clay	15.1026 kg	Dried clay	12.0515 kg
	Diesel burned in building machine	0.57385 Mj	Carbon dioxide, fossil	0.06267 kg
	Electricity, medium voltage	69.28 wh	Water (emission to air)	3.0510 kg
Grinding & dust removal	Dried clay	12.0515 kg	Clay powder	11.8100 kg

	Electricity, medium voltage	316.54 wh	Particulates, < 2.5 µm	0.22883 kg
Bagging of clay	Clay powder Kraft paper, unbleached Electricity, medium voltage	11.8100 kg 0.03543 kg 14.17 wh	Bag of clay	11.84543 kg
Transportation of clay	Bag of clay Transport, freight, lorry (330 km)	11.84543 kg 3.8973 t*km	Clay bag transported	11.84543 kg
Adsorption by clay	Clay bag transported Polluted water by lead Electricity, medium voltage	11.8100 kg 1.0 m3 256.7 wh	Waste water treated Polluted clay by Pb Lead	1.0 m3 11.8100 kg 0.005 kg
Polluted clay Transport to landfill	Polluted clay by Pb Transport to landfill (20 km)	11.84543 kg 0.2369 t*km	Polluted clay by Pb in landfill	11.84543 kg

Mechanical processing: crushing, grinding, and sieving, follows to achieve an optimal particle size for adsorption, requiring energy as an input and generating fine dust (e.g., PM10 or PM2.5) as outputs. Laboratory quality checks involve additional inputs like water and electricity, with minimal outputs beyond analytical waste. During the adsorption phase, inputs include contaminated water and the prepared clay, while outputs consist of purified water and metal-saturated clay residues requiring waste management.

For recycled debris (**Table 2**), the process begins with collection from the Hamici landfill in Algiers. Inputs include the RCD and energy for collection, with dust emissions as an initial output. The debris is transported by truck to the processing site, with fuel as an input and transport-related emissions (e.g., CO_2) as outputs.

Table 2: Life cycle inventory of RCD.

Process step	Inputs	Quantity (input)	Outputs	Quantity (output)
Crushing debris	Waste concrete	4.0239 kg	Crushed debris	3.9837 kg
	Electricity, medium voltage	9.29 wh	Particulates, < 10 µm	0.04024 kg
Grinding debris	Crushed debris	3.9837 kg	Powder debris	3.9300 kg
	Electricity, medium voltage	120.90 wh	Particulates, < 2.5 µm	0.04024 kg
Bagging debris	Powder debris	3.9300 kg	Bag of debris	3.94179 kg
	Kraft paper, unbleached	0.01179 kg		
	Electricity, medium voltage	4.716 wh		
Transportation of debris	Bag of debris	3.94179 kg	Bag of debris transported	3.9300 kg
	Transport, freight, lorry (20 km)	0.0788 t*km		
Adsorption by debris	Bag of debris transported	3.9300 kg	Treated water	1.0 m3
	Polluted water by lead	1.0 m3	Lead	0.001 kg
	Electricity, medium voltage	192.5 wh	Polluted concrete by Pb	3.9310 kg
Polluted Debris Transport to landfill	Polluted concrete by Pb	3.9310 kg	Polluted concrete by Pb in landfill	3.9310 kg
	Transport to landfill (20 km)	0.0786 t*km		

Mechanical preparation: crushing and sieving, optimizes particle size and adsorption efficiency, using energy as an input and producing fine dust (e.g., PM10 or PM2.5, potentially alkaline due to concrete) as outputs. Laboratory validation requires water and electricity, with minor waste outputs. In the adsorption stage, inputs comprise contaminated water (with lead) and the processed debris, while outputs include treated water and metal-saturated debris destined for disposal or potential reuse.

It should be noted that although preliminary batch adsorption tests were conducted at a controlled pH of 5.5 to prevent spontaneous metal precipitation and accurately determine adsorption kinetics and isotherms, chemical reagents such as HCl and NaOH were excluded from the industrial-scale life cycle inventory. As demonstrated by the pH effect study, the inherent basic nature of the RCD naturally drives the adsorption process under alkaline conditions (around pH 8-12 where optimal removal efficiencies are achieved. Therefore, no external chemical pH adjustment or final neutralization step is operationally required in a full-scale continuous application.

2.4.3 Life Cycle Inventory Background Database and System Model

The background life cycle inventory data were modeled using the ecoinvent database version 3.1 (reference year 2008), implementing the attributional "Allocation, cut-off by classification" system model. As detailed by Wernet et al. [37] this model maintains a strict boundary by assigning no environmental burdens to secondary materials entering the recycling chain, while fully attributing waste treatment burdens to the generating activity. To accurately represent local operating conditions, the national electric power generation mix for Algeria was specifically contextualized based on national utility data (Sonelgaz). The Algerian grid profile is heavily fossil-fuel reliant, with over 98% of national electricity generated from natural gas (open-cycle gas turbines, combined-cycle gas turbine (CCGT) units, and conventional steam boilers), while hydroelectricity (<1%) and solar PV (<1.5%) contribute marginally. This geographic specification ensures full compliance with the regionalization principles of ecoinvent v3 and prevents underestimation of grid-related environmental impacts during adsorbent preparation and batch operation

2.5.3 Environmental Impact Assessment

The environmental impacts of the natural clay and recycled debris processes were evaluated using the Life Cycle Impact Assessment (LCIA) methodology, utilizing OpenLCA software (version 2.5.0) and the ecoinvent 3.1 cutoff database. The environmental burdens were calculated using the harmonized ReCiPe method, which integrates both midpoint and endpoint indicators into a consistent modeling framework [38]. The ReCiPe Midpoint (H) approach was applied to assess specific environmental mechanisms, providing high scientific robustness and lower uncertainty for individual impact categories [39]. Furthermore, to facilitate decision-making and account for inherent modeling uncertainties, the impacts were aggregated at the endpoint level into three areas of protection: human health, ecosystem quality, and resource scarcity. The endpoint impacts were evaluated across three distinct cultural

perspectives: the Hierarchist (H/A) perspective, representing scientific consensus and medium-term horizons; the Individualist (I/A) perspective, based on short-term horizons and technological optimism; and the Egalitarian (E/A) perspective, which adopts a highly precautionary principle over a long-term time horizon [40].

3 Results and discussion

3.1 Characterization results

3.1.1 Results of the Morphological and Elemental Characterization (SEM/EDX)

Figures 7 and **8** presents the results the surface morphology and elemental composition of the raw clay and the RCD respectively, using Scanning Electron Microscopy coupled with Energy Dispersive X-ray Spectroscopy (SEM-EDX).

SEM micrographs of raw clay (**Figure 7**) reveal a heterogeneous, highly agglomerated structure composed of layered sheets and flaky tactoids. This micro-porous and rough surface morphology provides a high accessible surface area, which is structurally optimal for the diffusion and physical capture of heavy metal ions [41].

EDX quantitative analysis confirms an aluminosilicate framework dominated by O (48.30 wt%), Si (22.20 wt%), and Al (12.10 wt%). The resulting Si/Al mass ratio of 1.83 is characteristic of 2:1 phyllosilicate minerals, such as montmorillonite or illite [42]. The detection of structural Fe (4.83 wt%) and Mg (1.77 wt%) indicates isomorphic substitutions within the octahedral sheets. Furthermore, the presence of alkali and alkaline earth metals specifically: Ca (2.63 wt%), K (2.53 wt%), and Na (2.03 wt%), identifies the principal exchangeable interlayer cations. The abundance of these cations confirms that ion exchange is a primary driving mechanism for the adsorption process [43].

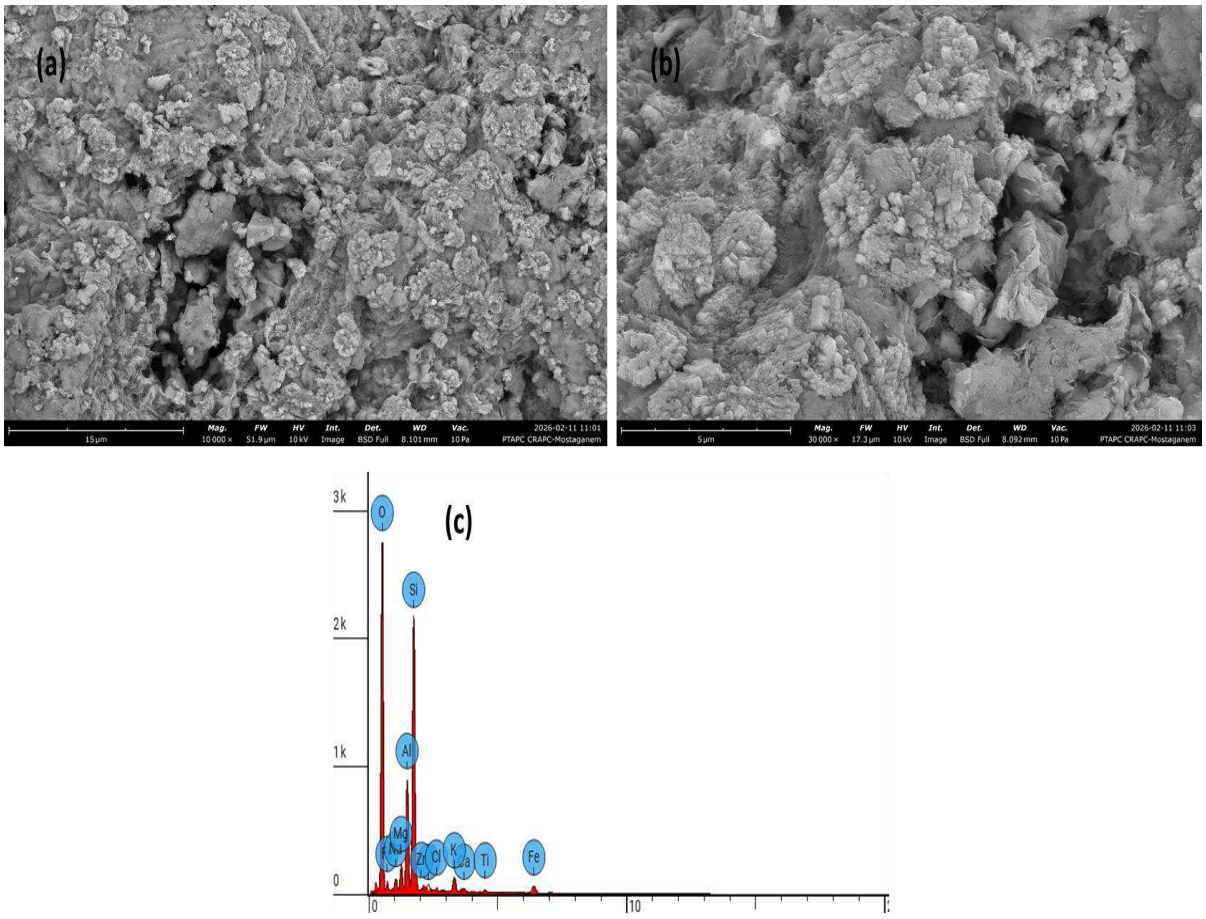

Figure 7: SEM/EDX micrograph of the studied clay: (a): clay (× 10000), (b): clay (×30000), and (c): chemical composition.

For the RCD, SEM micrographs (**Figure 8**) display an irregular, highly angular, and granular morphology. This fragmented and rough structure is typical of crushed cementitious waste, offering a highly heterogeneous surface with numerous active sites suitable for the physical and chemical binding of heavy metals.

Quantitative EDX analysis shows that the material is predominantly composed of O (50.62 wt%), Ca (29.06 wt%), and C (11.43 wt%). This elemental signature corresponds to the carbonated cement paste matrix inherent to RCD, rather than pure calcite crystallites. The presence of minor elements, including Si (2.40 wt%), Mg (1.70 wt%), Fe (1.27 wt%), and Al (1.23 wt%), reflects residual siliceous sand aggregates and unreacted cement phases. The high calcium content facilitates heavy metal removal primarily through surface complexation and ion exchange with the calcium-silicate-hydrate (C-S-H) phases, alongside the surface precipitation of lead as insoluble carbonate or hydroxide phases. These mechanisms, particularly the dominance of ion-exchange processes in calcium-rich cementitious matrices, have been validated in recent studies focusing on the adsorption performance of recycled concrete in aqueous systems [15].

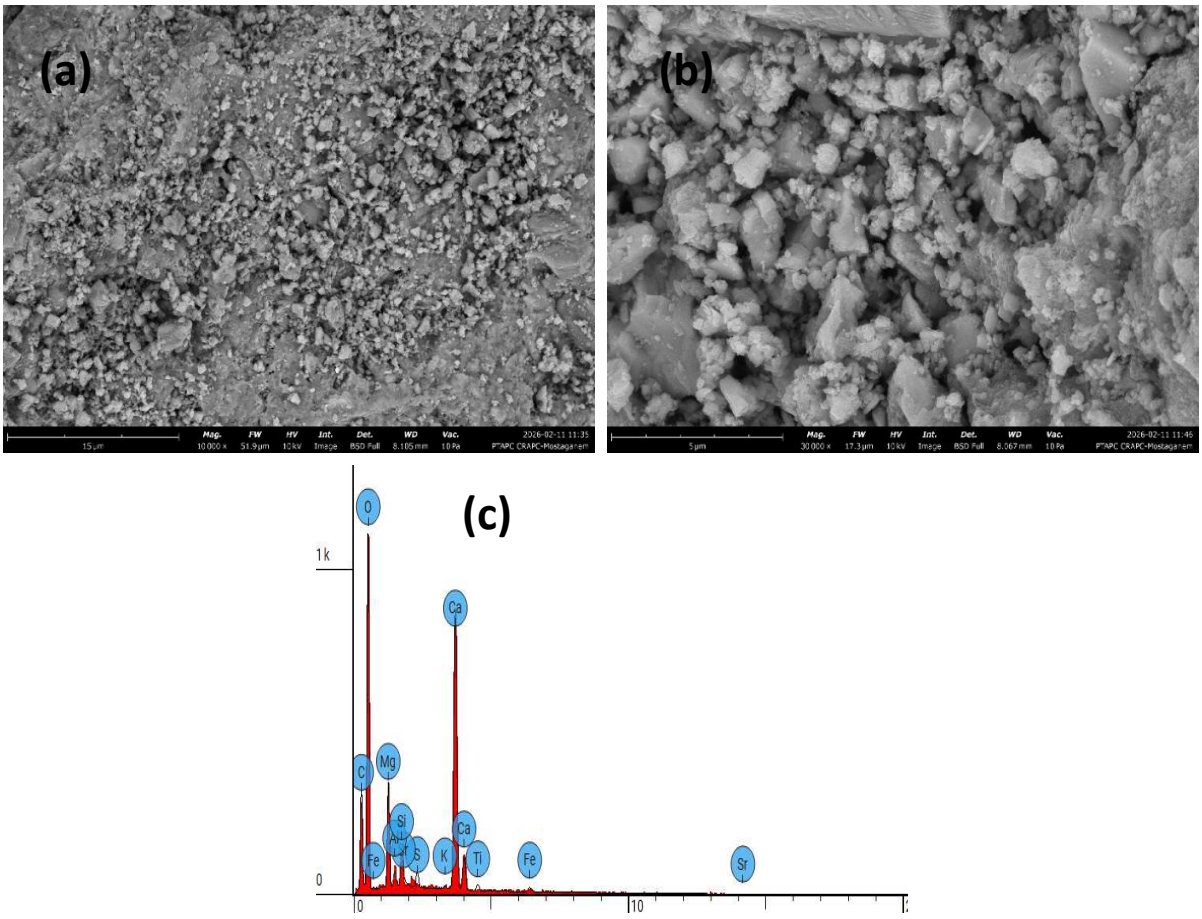

Figure 8: SEM/EDX micrograph of the studied recycled debris: (a) Recycled debris (× 10000), (b) Recycled debris (×30000), and (c) Chemical composition.

3.1.2 Results of the Thermogravimetric Analysis

Thermogravimetric analysis (TGA) was performed to evaluate the thermal stability and structural composition of the adsorbents (**Figure 9**).

The TGA curve of the clay sample exhibits a characteristic thermal profile for hydrated aluminosilicates, with a total mass loss of approximately 14% distributed across two main stages. The initial weight loss of 8% below 150 °C is attributed to the removal of physically adsorbed and loosely bound interlayer water [44]. A second thermal event occurs over a broader range between 400 and 650 °C, where a mass reduction of roughly 6% [45] This value aligns well with the 5–6% mass loss typically expected for the dehydroxylation of pure montmorillonite [46]. Furthermore, the absence of marked degradation above 650 °C confirms the lack of substantial calcite, which would otherwise decompose between 750 and 850 °C [47]. At 900 °C, the residual mass stabilizes at roughly 86%, reflecting the persistence of the refractory aluminosilicate framework.

In contrast, The TGA curve of the recycled debris shows a thermal behavior typical of a highly carbonated cementitious material. A first limited mass loss of about 1.35% between 25 and 200 °C is related to the evaporation of free water and the dehydration of calcium silicate hydrate phases [48], [49].

This is followed by a minor loss of approximately 1.0% between 400 and 500 °C, attributed to the dehydroxylation of residual portlandite, $Ca(OH)_2$. The low intensity of this event suggests that most of the calcium hydroxide had already been consumed by natural carbonation [50]. The most significant mass loss occurs between 600 and 800 °C, where a sharp decrease of 32% is recorded. This step is assigned to the decarbonation of calcite and dolomite, leading to the formation of CaO and MgO [51]. The remaining mass at 900 °C, approximately 65%, confirms the presence of thermally stable mineral phases, mainly silica derived from the aggregate skeleton [52].

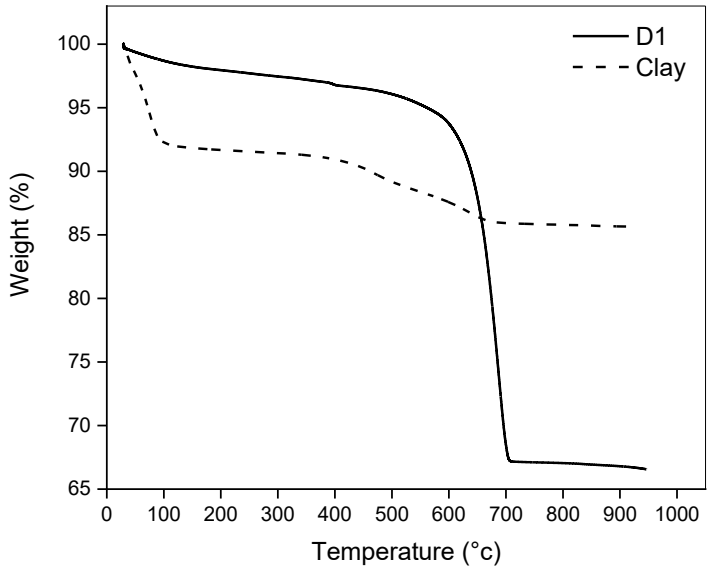

Figure 9. Thermogravimetric analysis (TGA) curves of the clay and recycled debris.

3.1.3 Results of the Particle Size Distribution

The particle size distributions of the adsorbents, determined by laser diffraction (**Figure 10** and **Table 3**), reveal distinct volumetric profiles. Bentonite clay (**Figure 10a**) exhibits a highly heterogeneous, trimodal distribution. Its dominant fraction lies in the submicron range (0.06–0.30 µm), typical of fine montmorillonitic materials [53], [54]. Secondary modes appear at 10–20 µm (intermediate silt or undispersed particles) and above 1000 µm (coarse agglomerates) [54]. Consequently, despite low D10 (0.101 µm) and D50 (0.164 µm) values, this massive coarse fraction significantly skews the overall statistics, leading to a high D90 (1864.7 µm) and mean diameter (450.88 µm) [55].

Conversely, the recycled debris (**Figure 10b**) displays a bimodal and considerably finer distribution. Its dominant ultrafine fraction closely mirrors that of the clay (D10 = 0.095 µm, D50 = 0.163 µm, D60 = 0.194 µm), indicating that over half the volume consists of particles smaller than 0.2 µm [56]. A broader secondary population around 10 µm constitutes the remaining fraction. The absence of massive agglomerates in the recycled debris results in a drastically lower D90 (12.39 µm) and mean particle diameter (3.90 µm) compared to bentonite [57]. Overall, while both materials share a highly active submicron fraction, the recycled debris provides a much finer and more homogeneous size profile.

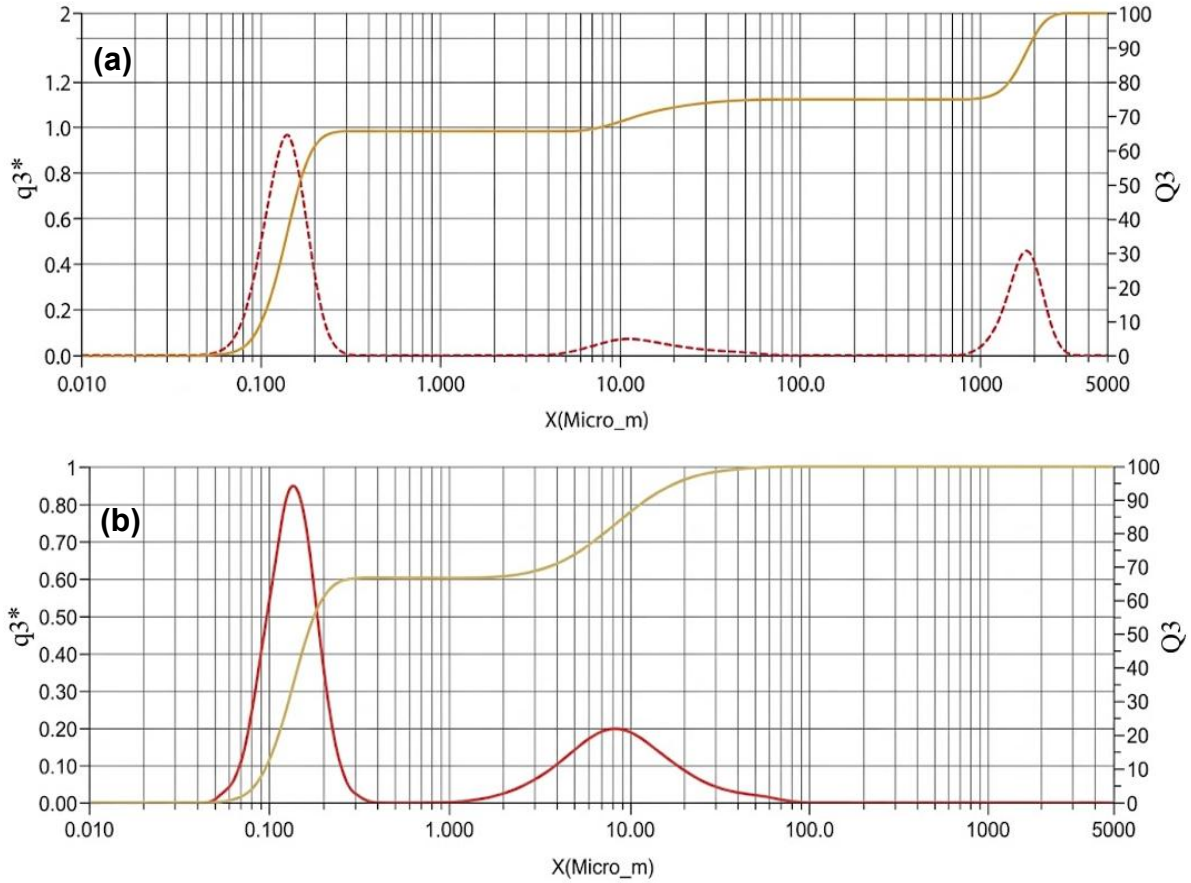

Figure 10. Particle size distribution curves of: (a) bentonite clay; (b) RCD.

Table 3. Particle size distribution parameters of recycled debris and bentonite clay.

Parameter	Recycled debris	Bentonite clay
D_{10} (µm)	0.095	0.101
D_{50} (µm)	0.163	0.164
D_{60} (µm)	0.194	0.193
D_{90} (µm)	12.39	1864.7
Mean diameter (µm)	3.90	450.88
Distribution type	Bimodal	Trimodal

3.2 Effect of parameters

3.2.1 Effect of mass

A study was carried out on the influence of the variation in the mass of the debris on the adsorption of the Pb^{2+} ion. The masses tested varied from 0.1 to 2 g, with an initial lead concentration set at 50 mg/L. The pH of the solution was maintained at 5.5 under agitation.

As illustrated in **Figure 11**, the lead removal efficiency of the recycled debris (D) rises sharply from 0.05 g to 0.2 g, reaching a peak of 90% between 0.2 g and 0.3 g, before slightly declining and stabilizing around 85–86% at higher masses (0.4–1.2 g). In contrast, clay (C) exhibits a more gradual, steady increase in lead sorption, starting from approximately 47.7% at 0.05 g and requiring a dosage of 0.6 g

to reach its maximum efficiency of 90.2%. Notably, the recycled debris achieves its optimal lead removal performance at less than half the mass required by clay (0.2–0.3 g vs. 0.6 g). This rapid attainment of peak efficiency highlights the environmental superiority of the recycled material, as it significantly minimizes both adsorbent consumption and the subsequent generation of contaminated solid waste. While the performance of clay progressively depends on higher mass additions, the recycled debris demonstrates high efficacy at low dosages combined with operational stability across a broad mass range.

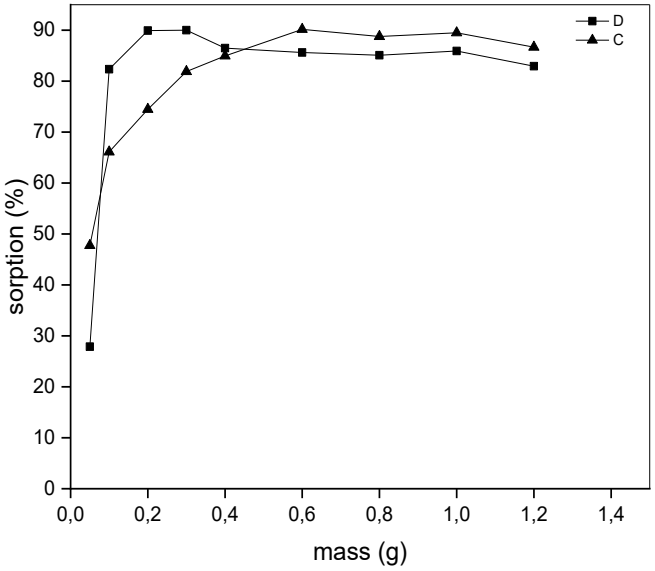

Figure 11. Effect of adsorbent dosage on removal efficiency and adsorption capacity of Pb^{2+}

3.2.2 Effect of pH

This comparative study examines the influence of pH on lead removal using two adsorbents: natural clay and recycled basic debris (**Figure 12**). While clay demonstrates superior efficiency in slightly acidic to neutral environments (pH 4–7), the recycled debris excels markedly in basic conditions, achieving a removal rate exceeding 96% at pH 12.

It is noteworthy that the debris inherently possesses a high pH=12, unlike clay, which has a near-neutral pH=8. In industrial settings, adjusting pH to acidic levels entails significant technical and economic costs. The use of recycled debris thus offers a dual advantage: it eliminates the need for pH-correcting reagents and optimizes performance under basic conditions. These properties position the recycled debris as a strategic alternative for industrial processes, combining efficiency in alkaline environments with reduced chemical inputs while aligning with sustainability imperatives.

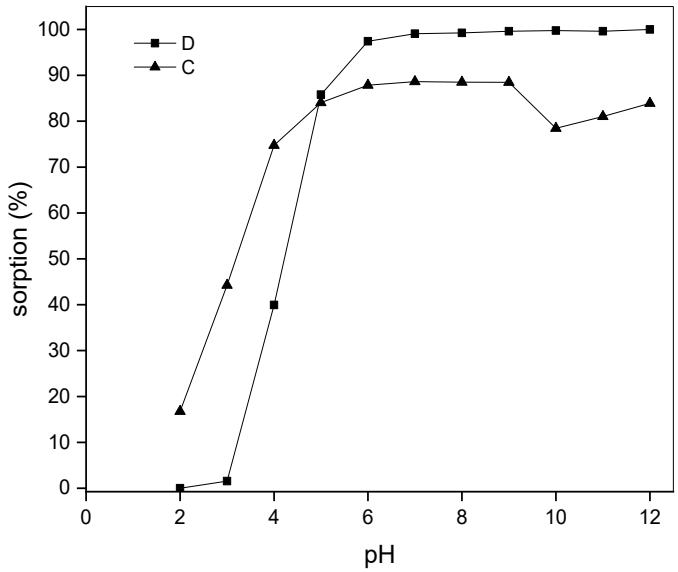

Figure 12. Effect of pH on removal of Pb^{+2} by debris and clay.

The suitability of the treated effluents for potential discharge was evaluated against the regulatory threshold of 1 mg/L specified by the Algerian Executive Decree 93-160. Starting from an influent concentration of 50 mg/L, the RCD-based system achieves a high removal efficiency of 99% under basic pH conditions (**Figure 12**), successfully reducing the residual Pb^{2+} concentration to the required discharge limit of 1 mg/L. Conversely, the clay-based system yields a 90% removal efficiency, resulting in a residual concentration of 5 mg/L, which exceeds the regulatory limit. Consequently, while RCD can be directly discharged or integrated into an environmental profile without further polishing, the clay system would require a complementary secondary treatment step to meet local discharge standards. This discrepancy underscores the technological advantage of RCD, which combines favorable environmental life cycle impacts with direct regulatory compliance.

3.2.3 Effect of concentration

Figure 13 illustrates the effect of initial Pb^{2+} concentration (10–100 ppm) on the sorption efficiency of the recycled debris (D) and clay (C). The recycled debris exhibits remarkable performance at lower concentrations, achieving complete removal (100% efficiency) of Pb^{2+} between 10 and 40 ppm. This optimal sorption indicates an abundance of readily available active sites on the material's surface, which easily accommodate and sequester the lead ions present in the solution. As the initial concentration increases from 50 to 100 ppm, the removal efficiency of D gradually declines to approximately 83%. This expected trend is directly attributed to the progressive saturation of the active adsorption sites relative to the increasing number of Pb^{2+} ions in the aqueous phase.

Conversely, the clay sample displays a lower initial sorption efficiency of roughly 45% at 10 ppm, which steadily increases to plateau near 85% at 40–50 ppm. While clay experiences minor fluctuations at higher concentrations, both adsorbents eventually converge to a similar removal efficiency (83–85%) at

464 the maximum tested concentration of 100 ppm. Overall, while both materials perform comparably at
465 high pollutant loads, the recycled debris demonstrates a clear and significant superiority in treating low-
466 to-moderate Pb^{2+} concentrations, ensuring complete environmental remediation.

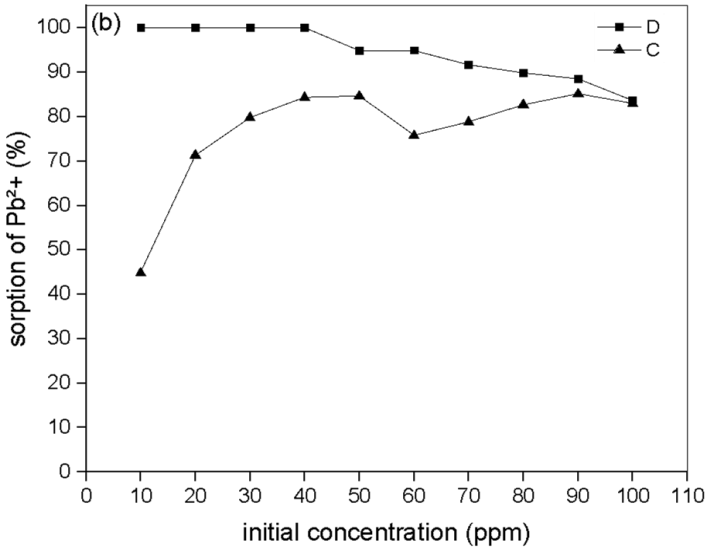

467
468 **Figure 13.** Effect of initial metal concentration on removal efficiency of Pb^{2+} by debris and clay.

469 **3.2.4 Contact time**

470 **Figure 14** depicts the effect of contact time on the sorption efficiency of Pb^{2+} by the recycled debris (D)
471 and clay (C) over a 60-minute period. Both materials exhibit extremely rapid initial adsorption kinetics,
472 characteristic of a high affinity between the heavy metal ions and the adsorbent surfaces.
473 Notably, the recycled debris (D) demonstrates an outstanding ultrafast uptake, removing approximately
474 93% of Pb^{2+} within the first 5 minutes and reaching a peak efficiency of nearly 98% at 15 minutes. This
475 near-instantaneous response suggests that the adsorption process on the recycled debris is predominantly
476 surface-driven, indicating that its active sites (such as carbonates and calcium silicate hydrates) are
477 readily and entirely accessible without significant intra-particle diffusion limitations.
478 In comparison, the clay (C) also shows fast kinetics, achieving about 88% removal at 5 minutes, but
479 requires a slightly longer contact time (approximately 20 minutes) to reach its maximum and highly
480 stable equilibrium plateau of 98–99%. While the clay maintains this plateau throughout the 60-minute
481 duration, the recycled debris exhibits slight fluctuations and a minor decrease in sorption efficiency
482 towards the end of the run (dropping to 82% at 60 minutes). This behavior may be attributed to a
483 dynamic re-equilibration between the solid and liquid phases or localized pH variations at the solid-
484 solution interface.

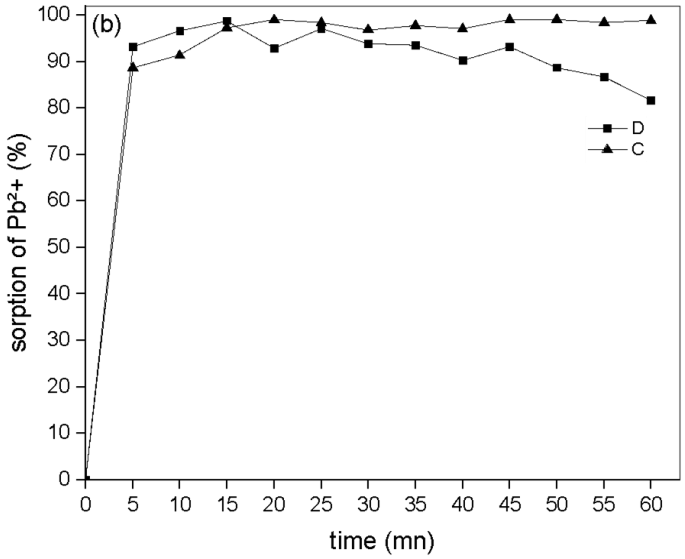

485

486 **Figure 14.** Effect of contact time on the removal efficiency of Pb^{2+} by clay and debris.

487 To reach residual concentrations compliant with regulatory standards (< 1 mg/L), the initial batch
488 treatment which achieves a 90% removal efficiency (i.e., 5 mg/L residual from an initial concentration
489 of 50 mg/L in a single stage) can be optimized through a sequential treatment with multiple successive
490 adsorption cycles. Thanks to the high cation exchange capacity of the materials, this multi-stage
491 configuration provides a straightforward solution to ensure strict compliance with discharge limits
492 without requiring excessive reagent consumption.

493 **3.3 Kinetic Modeling**

494 As shown in **Figure 15** and **Table 4**, the pseudo-second-order model provided an excellent fit to the
495 experimental data for adsorption of Pb^{+2} onto clay and recycled debris, with very high correlation
496 coefficients ranging from 0.999. In addition, the calculated q_e values were in close agreement with the
497 experimental ones, confirming the suitability of this model for describing the adsorption kinetics. These
498 results suggest that the adsorption process is mainly controlled by surface-related interactions involving
499 the availability of active sites on the adsorbent and the concentration of metal ions in solution [57,58].
500 The kinetic parameters detailed in **Table 4** further demonstrate that RCD exhibits a substantially higher
501 adsorption capacity than clay.

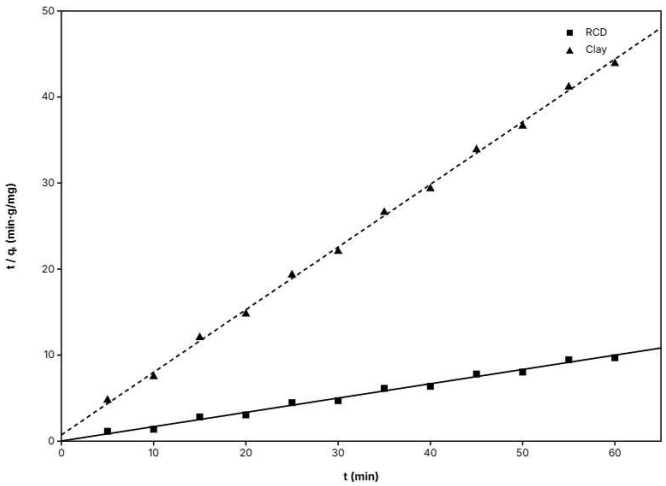

Figure 15. Plot of the second-order kinetic model for Pb^{2+} onto clay and recycled debris.

Table 4. Parameters of the pseudo-second-order kinetic model for Pb^{2+} adsorption onto the two adsorbents.

		Adsorbent	
Equation	$\frac{t}{q_t} = \frac{1}{K_2 q_e^2} + \frac{1}{q_e}$	Clay	Debris
Parameters	q_e (exp) (mg/g)	1.365	5.957
	q_e (cal) (mg/g)	1.374	6.017
	K_2 ($g.mg^{-1}.mn^{-1}$)	0.728	1.103
	R^2	0.999	0.999

3.4 Adsorption Isotherm Studies

Equilibrium adsorption data were analyzed by applying four isotherm models: Langmuir, Freundlich, Temkin, and Dubinin-Radushkevich (D-R). The obtained results are presented in **Table 5** and **Figure 16**.

The comparative analysis of Pb^{2+} adsorption on the two studied adsorbents, clay and debris, reveals significant differences in their adsorption performance and affinity toward these metal ions.

Pb^{2+} adsorption onto clay aligns best with the Temkin model ($R^2 = 0.97$), emphasizing the prominent role of adsorbate-adsorbate interactions.

In contrast, the recycled debris system exhibits a highly homogeneous surface behavior, where Pb^{2+} adsorption is perfectly fitted by the Langmuir model ($R^2 = 0.99$). The debris demonstrates a remarkable maximum monolayer capacity (q_m) for Pb^{2+} of 12.13 mg/g, significantly outperforming the clay's capacity (5.00 mg/g).

Finally, the Dubinin-Radushkevich model confirms the thermodynamic nature of these interactions: the mean free energy (E) values for all systems range from 0.70 to 5.87 kJ/mol. Because these values remain strictly below 8 kJ/mol, the overall removal process is definitively governed by physical adsorption (physisorption) across all studied conditions.

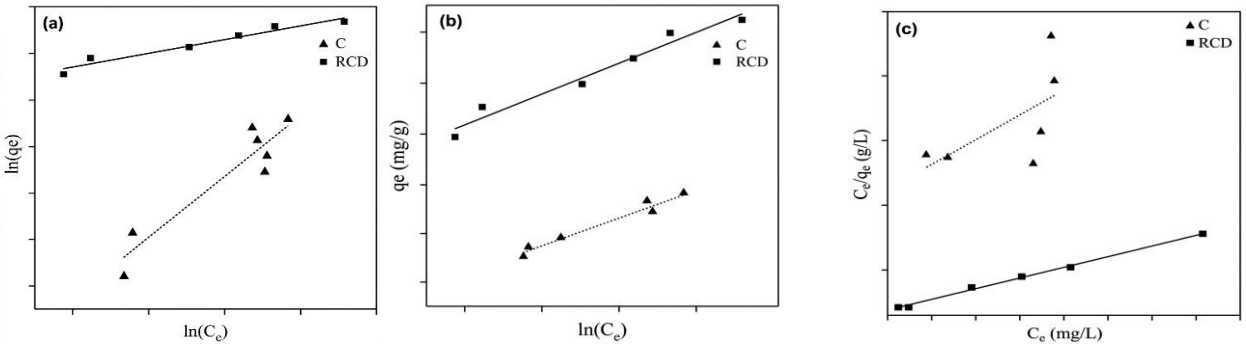

Figure 16. Adsorption isotherms of: (a) Freundlich, (b) Temkin, and (c) Langmuir, onto the two adsorbents.

The batch experiments were conducted using a solution volume of V = 0.05 L (50 mL) at an initial lead concentration of C_0 = 50 mg/L.

RCD: At a dosage of m = 0.2 g we achieved 98% removal efficiency.

$$\text{Dosage}_{RCD} = \frac{m_{lab}}{V_{lab}} = \frac{0{,}20g}{0{,}05L} = 4{,}0\ Kg/m^3$$

$$M_{max,RCD} = 4000 \times 12{,}14 = 49600mg = 49{,}6\ g > 49\ g\ Pb$$

Clay: At a dosage of m = 0.6 g, we achieved 90% removal efficiency.

$$\text{Dosage}_{C} = \frac{m_{lab}}{V_{lab}} = \frac{0{,}60g}{0{,}05L} = 12{,}0\ Kg/m^3$$

$$M_{max,RCD} = 11810 \times 5{,}00 = 59050mg = 59{,}05\ g > 45\ g\ Pb$$

Table 5. Summary table of isotherm parameters for Pb^{+2} adsorptions on debris and clay.

Isotherm	Parameter	Unit	Value Pb^{+2}	
			Clay	Debris
Temkin	KT	L/g	0.42	4.02
	bT	KJ/mol	2.35	2.38
	R^2	-	0.97	0.96
Langmuir	qm	mg/g	5.00	12.13
	RL	-	0.15	0.05
	KL	L/g	0.11	0.39
	R^2	-	0.94	0.99
Freundlich	N	-	0.76	3.41
	Kf	-	0.14	4.80
	R^2	-	0.88	0.95
Dubinin Radushkevich	qm	mg/g	4.48	9.96
	β	mol^2/J^2	6.62×10^{-7}	7.98×10^{-7}
	E	KJ/mol	0.70	0.79
	R^2	-	0.76	0.92

3.5 Results of Life Cycle Analysis (LCA)

3.5.1 Life Cycle Impact Analyses Results: Midpoint (H)

The functional unit is defined as the treatment of 1.00 m^3 of water polluted with Pb^{2+} using 0.2 g of RCD (achieving a 98% removal efficiency, derived from the pH effect - **Figure 11**) and 0.6 g of clay (achieving a 90% removal efficiency, derived from the pH effect - **Figure 11**), with the adsorbent mass dosages determined from the mass effect evaluation (**Figure 10**). In accordance with ISO 14044 [36], this functional unit ensures functional equivalence by coupling the volume of water with the actual mass performances and removal efficiencies of each material.

These laboratory-scale adsorbent masses were extrapolated to the industrial scale (1 m^3) by applying geometric similitude and scale factor criteria. This leads to required mass values of 3.93 kg for RCD and 11.81 kg for clay.

The environmental profiles of the two adsorbents were first evaluated at the midpoint level using the ReCiPe (H) methodology to identify the specific environmental mechanisms driving the impacts. The comparative assessment reveals a significant environmental advantage for RCD over natural clay across most impact categories. The comparative midpoint impacts are synthesized in **Figure 17**.

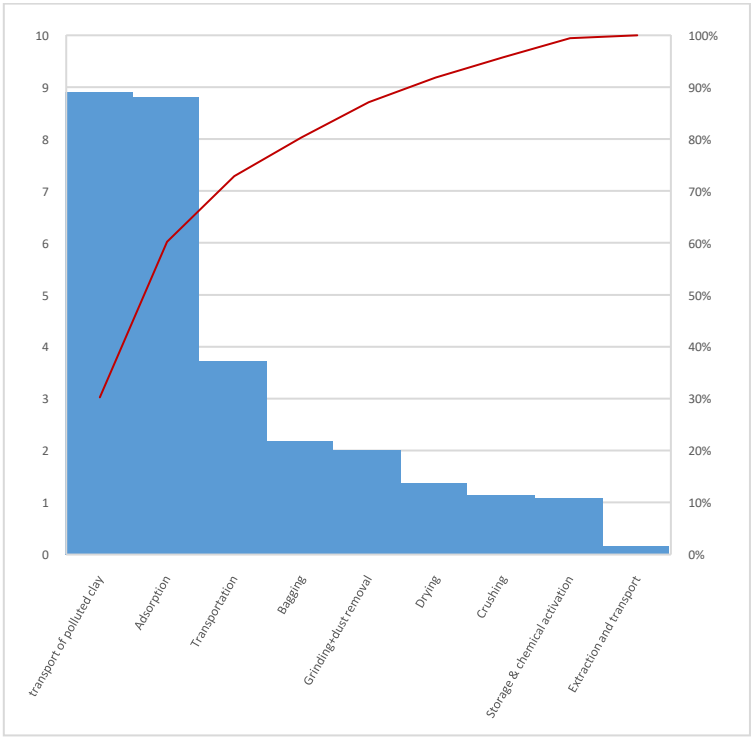

(a) Clay

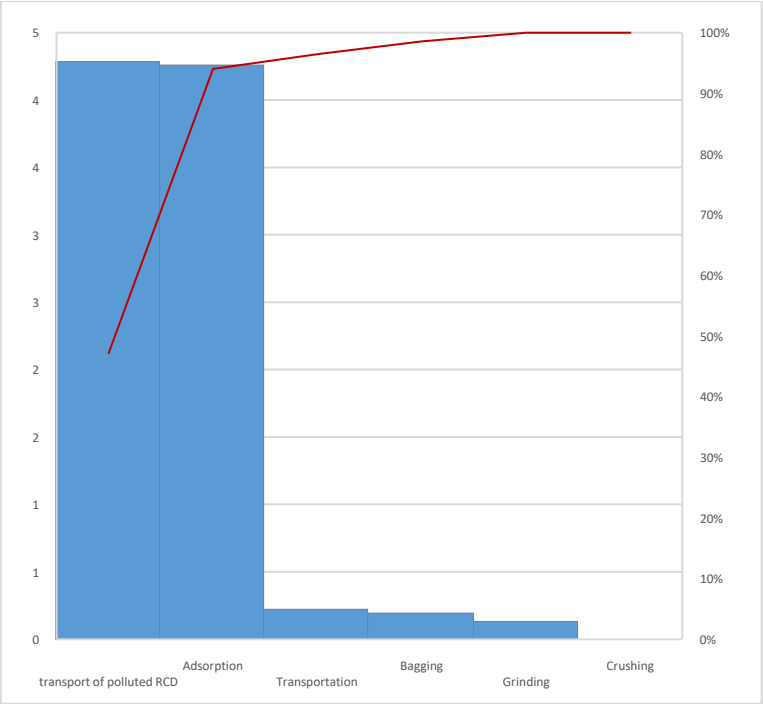

(b) RCD

Figure 17: Analysis of contributions and cumulative impacts by process step.

Figure 17 corresponding to Pareto charts, show the individual and cumulative impact of each process step: (a) for Clay and (b) for RCD. For both materials, the transport steps (notably the transport of materials and polluted clay) and the adsorption step clearly dominate the overall balance. Together, they account for the vast majority of cumulative impacts, exceeding 70%. In contrast, the upstream physical transformation steps (such as crushing, drying, grinding, or bagging) have marginal contributions to the overall impact.

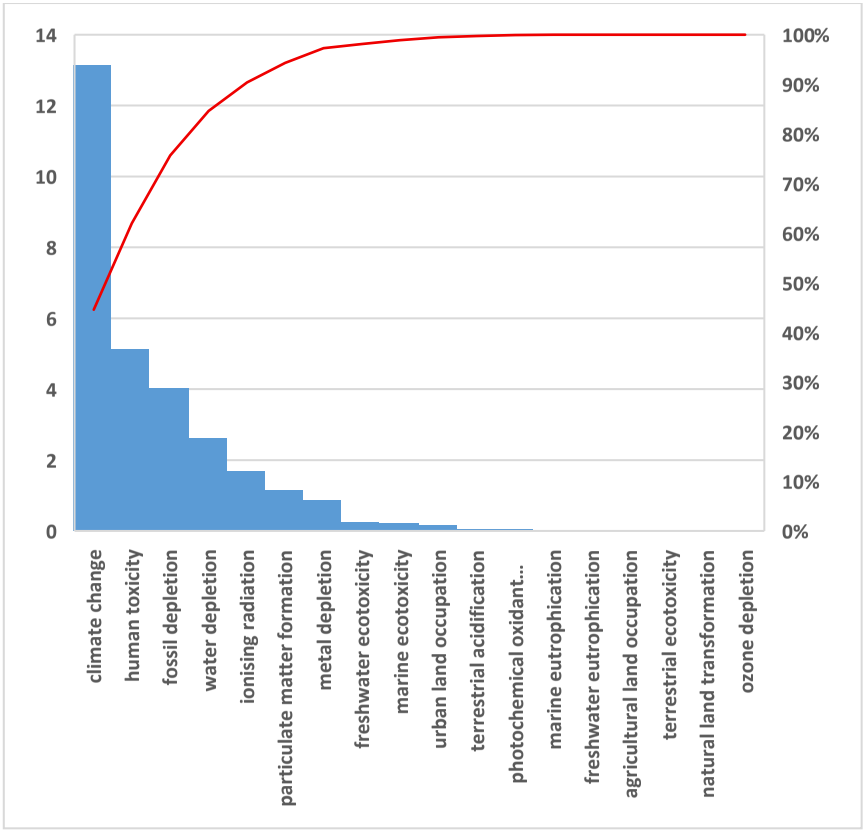

562

563 (a) Clay

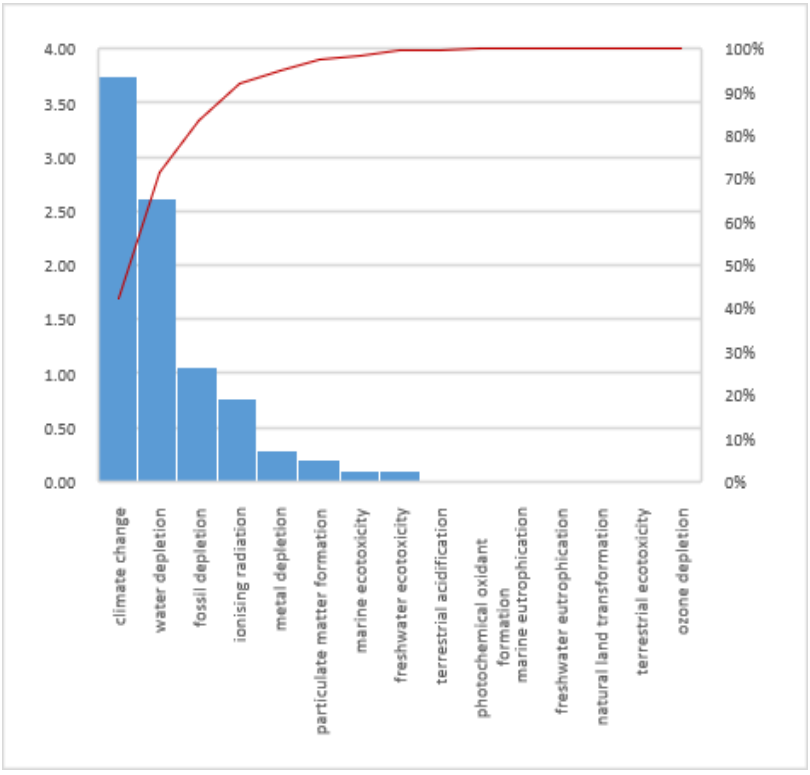

564

565 (b) RCD

566 **Figure 18:** Relative and cumulative contributions of environmental impact categories.

Figure 18 rank the different environmental impact categories (according to the ReCiPe method): (a) for Clay and (b) for RCD. For both clay and RCD, the climate change category is by far the most impactful, accounting on its own for the predominant share of the overall score. It is followed by other significant categories such as human toxicity, water depletion, or fossil depletion. It should be noted that the impacts of the different categories related to the clay-based process are about three times higher than those of the RCD-based process.

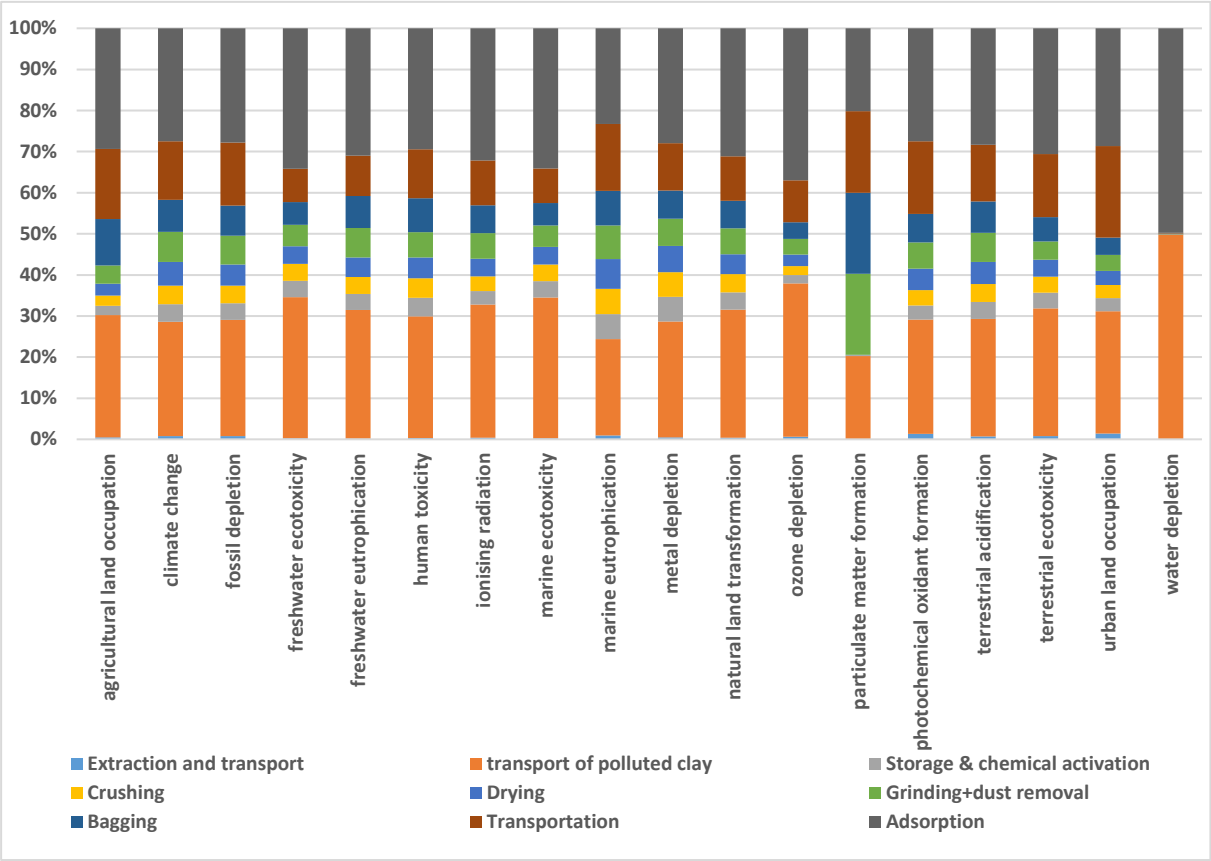

(a) Clay

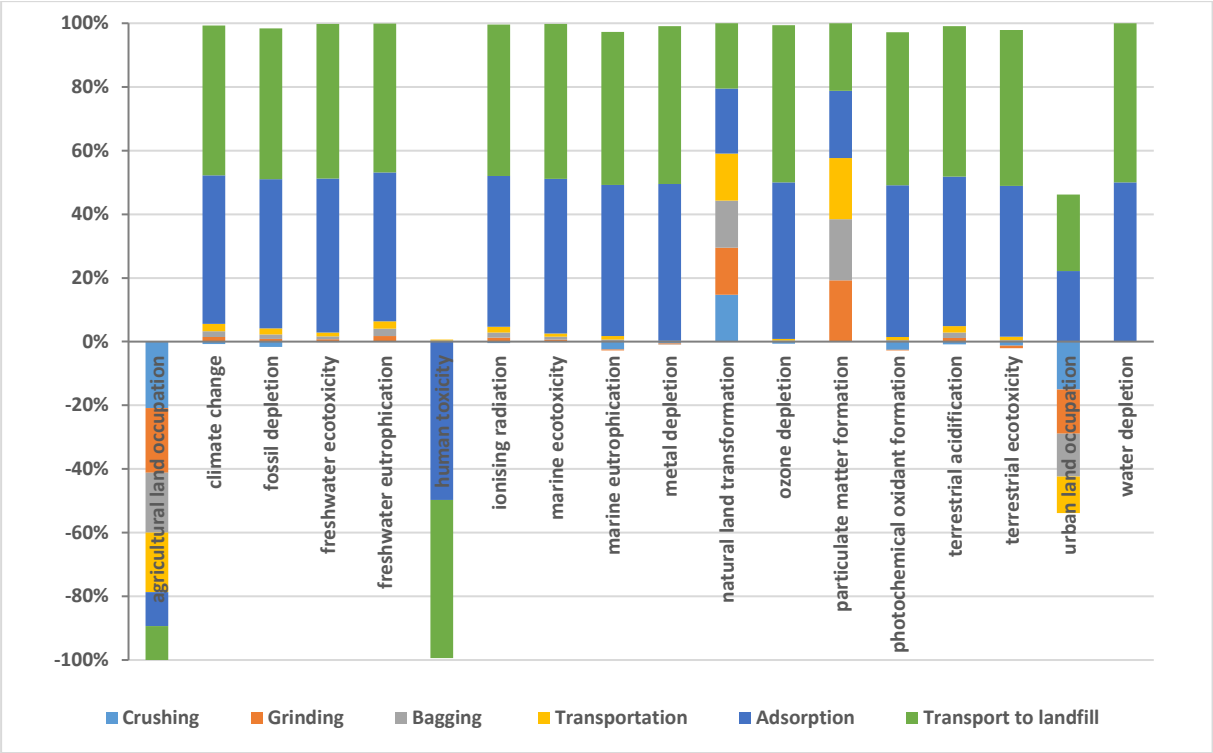

(b) RCD

Figure 19: Relative contribution (%) of the different process stages to environmental impacts (ReCiPe Method).

Figure 19 shows the percentage breakdown of each life cycle stage (extraction, transport, chemical activation, drying, grinding, adsorption, etc.) across all impact categories of the ReCiPe method. It makes it possible to precisely identify which sub-operations weigh the most heavily on a given indicator. Climate change, for instance, is primarily attributable to fuel consumption during the transport phase, as well as fossil energy consumption during the adsorption phase and the transport of polluted clay. For Climate Change: The impact is mainly dominated by the adsorption phase (~27% for clay vs. ~48% for debris) and the residues from the adsorption phase (~28% for polluted clay vs. ~46% for saturated RCD). For Fossil Depletion: The transport of polluted residues (~30% for clay vs. ~46% for RDC) and adsorption (~28% for clay vs. ~48% for debris), as well as the fuel consumption associated with clay transport (~15%), are the main drivers of this impact category.

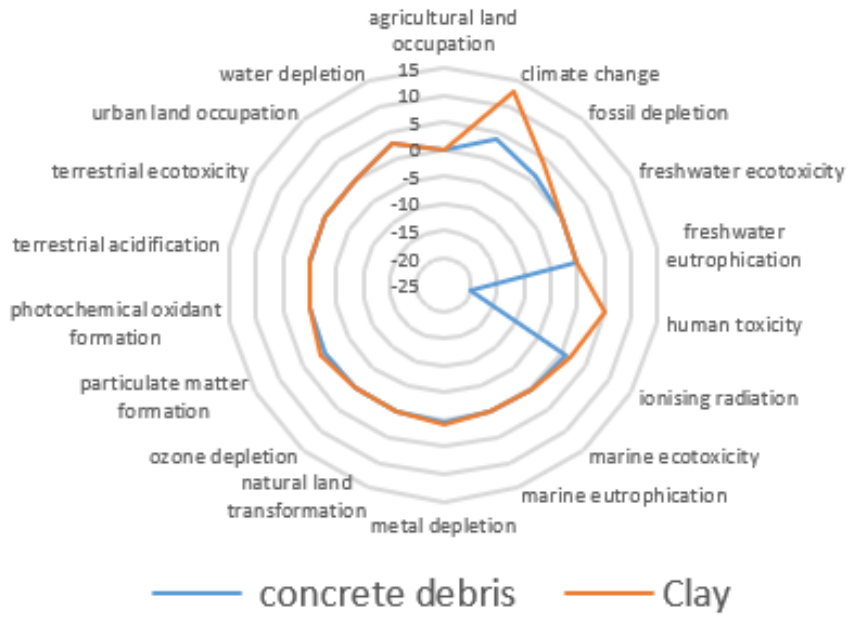

589

590 **Figure 20.** Radar diagram of Comparative midpoint impact assessment result

591 This radar chart in **Figure 20** highlights the environmental performance of concrete debris (blue line)
592 and clay (orange line) across all midpoint impact categories (climate change, resource depletion,
593 toxicity, etc.). This graphically demonstrates the environmental advantage of using alternative materials
594 derived from RCD over conventional natural materials (such as clay) for adsorption applications.
595 As detailed in this comparative analysis, the RCD system outperforms the natural clay system in 17 out
596 of the 18 evaluated environmental categories. The Global Warming Potential (climate change)
597 associated with the natural clay system reaches 2.25 kg CO_2-Eq, whereas the RCD system effectively
598 curbs this profile to 1.58 kg CO_2-Eq. This disparity is fundamentally rooted in the materials' respective
599 supply chains. The requisite thermal activation for clay cannot be considered a low-temperature process;
600 consequently, the heavy fossil fuel consumption required to maintain kiln temperatures drive the fossil
601 depletion indicator to 0.686 kg oil-Eq for clay, compared to only 0.455 kg oil-Eq for the mechanically
602 processed RCD.
603 The most critical divergence between the two matrices occurs within the human toxicity indicator. While
604 the natural clay system registers a positive burden of 2.14 kg 1,4-DCB-Eq, the RCD system yields a
605 highly significant negative impact of -9.06 kg 1,4-DCB-Eq. This negative value represents a substantial
606 environmental credit. By repurposing un-functionalized construction debris, the system avoids the toxic
607 emissions and leachate risks inherently associated with the conventional landfilling of CDW.
608 Crucially, throughout the batch adsorption phase, the pH was maintained strictly constant across all
609 tested sorbent quantities. This rigorous experimental constraint isolates the chemical capacity of the
610 adsorbents from pH-induced precipitation artifacts. Under these controlled conditions, the intrinsic
611 properties of the RCD, specifically the active CaO and SiO_2 phases, facilitated efficient lead
612 immobilization without generating secondary environmental burdens. Water depletion remained one of

the singular categories demonstrating near parity, consuming approximately 1.30 m^3 across both scenarios, governed entirely by the identical aqueous batch medium requirements.

3.5.2 Life Cycle Impact Analyses Results: Endpoint

To aggregate the localized midpoint mechanisms into overarching Areas of Protection (Human Health, Ecosystem Quality, and Resources), an endpoint assessment was executed. Endpoint assessment translates midpoint impact categories into damage indicators that are more directly interpretable in terms of real-world consequences, such as the loss of life years due to toxicity exposure, species extinction due to ecotoxicity, or resource scarcity costs.

The endpoint analysis is conducted across three distinct cultural perspectives within the ReCiPe framework: the Hierarchist (H), Individualist (I), and Egalitarian (E) worldviews. These perspectives differ in their time horizons, assumptions about technological change, and attitudes toward precaution. By testing all three perspectives, the analysis satisfies ISO 14044 [36] requirements for a sensitivity check and ensures that conclusions are robust across reasonable variations in methodological assumptions, the results of the three perspectives are summarized in **Table 6** [40].

Table 6 presents the unweighted life cycle damage assessment results across the three ReCiPe 2008 Areas of Protection (Human Health in DALY, Ecosystem Quality in species·yr, and Resources in USD 2000 surplus cost) evaluated across the Hierarchist (H), Individualist (I), and Egalitarian (E) cultural perspectives.

The endpoint analysis reveals that the RCD route consistently outperforms the bentonite clay system across all three protection areas regardless of the cultural perspective considered. Under the baseline Hierarchist perspective (H), the clay system induces a Human Health damage of 5.2010-2DALY, which is nearly an order of magnitude (9.6) higher than that of RCD (5.4210-3DALY). This marked disparity is primarily governed by respiratory effects associated with particulate matter formation (PM2.5 and PM10), exacerbated by the larger mass throughput required for clay (11.81 kg vs. 3.93 kg) and direct fossil combustion emissions during rotary thermal drying.

Regarding Ecosystem Quality, the bentonite clay system inflicts double the species loss compared to RCD, displaying an extraordinarily robust ratio of approximately 2.0 across all three cultural perspectives. This ecological damage is driven by highway freight emissions associated with inter-regional transport from the Mostaganem quarry to Algiers (330 km) compared to localized metropolitan sourcing for RCD (20km), alongside thermal drying greenhouse gas releases.

Similarly, the resource scarcity surplus cost for clay is 2.15 greater than that of RCD, directly reflecting virgin mineral extraction and higher fossil energy depletion. In full compliance with ISO 14044 [36] Clause 4.4.5, these unweighted endpoint characterizations confirm the overwhelming environmental superiority of valorizing concrete demolition waste as an eco-efficient circular adsorbent for industrial wastewater remediation

Table 6. Endpoint impact assessment results (per functional unit: 1 m³ treated wastewater).

Area of Protection	Unit	Adsorption by RCD			Adsorption by clay		
		(H,A)	(I,A)	(E,A)	(H,A)	(I,A)	(E,A)
Human health	DALY	0.0054219	0.010238138	0.00146475	0.052042025	0.049138	0.040367038
Ecosystem quality	Species. yr	9.35655E-06	1.01261E-05	2.12411E-05	0.000018981	2.01E-05	4.20945E-05
Resources	$	16.636285	18.78823	16.636285	35.838635	39.48684	35.838635

This study conducted a rigorous, ISO 14040 [30] and ISO 14044 [36]-compliant comparative LCA to evaluate the environmental viability of substituting natural clay with RCD for the removal of Pb^{2+} in aqueous batch systems. The integration of both Midpoint and Endpoint (ReCiPe 2008) impact assessments yields a definitive conclusion: the utilization of un-functionalized RCD provides a profound and robust environmental advantage over traditional natural clay.

At the midpoint level, the RCD system substantially mitigated Climate Change and Fossil Depletion impacts. This reduction is primarily achieved by bypassing the energy-intensive extraction and thermal activation processes required for clay minerals, a phase that strictly cannot be classified as a low-temperature operation. Furthermore, the repurposing of construction and demolition waste transformed the Human Toxicity impact from a net burden into a significant environmental credit, reflecting the avoided emissions of conventional landfilling. Importantly, because the experimental pH was maintained strictly constant across all tested quantities, the heavy metal removal efficiency is demonstrably attributed to the intrinsic active CaO and SiO_2 phases within the RCD matrix, validating its standalone chemical efficacy.

3.5.3 Uncertainty Analysis by Monte Carlo Simulation

To evaluate model robustness beyond mere qualitative variation of ReCiPe, a stochastic uncertainty analysis was executed using Monte Carlo simulation in OpenLCA (v2.5.0) (**Table 7)**. Key input parameters including unit process material quantities, transportation distances, grid emission factors, and background dataset values were assigned lognormal probability distributions characterized by their geometric mean (μ) and geometric standard deviation (σ_g), parametrized according to the ecoinvent v3 Pedigree matrix approach as detailed by Wernet et al. [37]. Monte Carlo simulation was conducted for both the RCD and Bentonite Clay systems across the primary endpoint Areas of Protection (Human Health, Ecosystem Quality, and Resource Scarcity), following the methodological guidelines established by the procedural requirements of ISO 14044 [36].

Table 7. Stochastic Monte Carlo uncertainty analysis.

Area of protection	Material	Mean value	95% Confidence Interval	CV (%)	Probability (RCD< Clay)
Human Health *(DALY)*	RCD	5.42×10^{-3}	$[4.75 \times 10^{-3}, 6.10 \times 10^{-3}]$	12.4%	99.8%
	Clay	5.20×10^{-2}	$[4.23 \times 10^{-2}, 6.17 \times 10^{-2}]$	18.6%	
Ecosystem Quality *(species·yr)*	RCD	9.36×10^{-6}	$[7.82 \times 10^{-6}, 1.12 \times 10^{-5}]$	14.1%	99.4%
	Clay	1.90×10^{-5}	$[1.54 \times 10^{-5}, 2.31 \times 10^{-5}]$	17.3%	
Resource Scarcity *(USD 2000)*	RCD	\$16.64	[\$14.20, \$19.10]	11.8%	100.0%
	Clay	\$35.84	[\$30.15, \$41.80]	15.2%	

RCD yielded lower Human Health damage than clay. The negative toxicity credit (avoided landfill burden) associated with RCD remained robustly negative, aligning with findings on construction waste diversion benefits by Knoeri et al. [58]. The Monte Carlo simulation confirms that the comparative environmental superiority of Recycled Concrete Debris over Natural Bentonite Clay is statistically significant ($p < 0.001$) and fully robust against operational, spatial, and inventory data uncertainties.

Key hydrodynamic-related parameters such as volumetric power input (P/V), impeller configuration, aeration strategy, and maximum gas sparge rate, as well as an appropriate feeding strategy, must be carefully selected to improve production yields in bioreactor. In this study, the feeding regimen was found to have an important impact on cell growth and productivity of a cumate-inducible CHO fed-batch cell culture. A low- volume feeding regimen avoided a rapid increase in osmolality, allowing for prolonged cell viability and a 33% increase in volumetric titer compared to the high-volume feeding regimen. Both sparged air and oxygen were used for dissolved oxygen (DO) control, utilizing three levels of airflow rates. An optimum airflow rate of 0.0031 vm was found to improve cell growth, longevity, and thus final titer. A larger air cap required increased gas flow rates, which led to an earlier cell mortality. Scale-up from 1-L to 10-L bioreactor using constant P/V and air cap volumetric gas flow rate (vm) allowed for comparable cell growth and productivity. Further investigation of the effect of mixing and aeration was done by maintaining P/V and vm constant throughout the cell culture, which further improved product titers at 11 days after induction. Our study also demonstrates that keeping a constant volume by removing a culture amount equal to the feed volume added at each sampling event can significantly improve the final volumetric titer. This finding shows the benefit of developing a concentrated feed to reduce the volume increase, which in turn could greatly ease the scale-up task.

4 Conclusion

Sustainable wastewater remediation increasingly relies on developing eco-friendly adsorbents that align with circular economy principles while minimizing cradle-to-gate environmental footprints. This study demonstrates that Recycled Concrete Debris (RCD) represents a highly effective and environmentally sustainable alternative to natural bentonite clay for lead (Pb^{2+}) removal from aqueous solutions.

Physicochemical characterization revealed that RCD possesses a significantly finer, more homogeneous particle distribution (mean size 3.90 μm) and a calcium-rich cementitious matrix (29.06 wt% Ca) that enables multi-modal retention, including C-S-H ion exchange, surface complexation, and carbonate/hydroxide precipitation. In batch adsorption experiments, RCD outperformed natural clay by achieving complete Pb^{2+} removal (100% at 10-40 ppm) at less than half the required dosage (0.2-0.3 g vs. 0.6 g). Moreover, the inherent alkalinity of RCD (pH ≈ 12) enables rapid treatment of basic industrial effluents without requiring chemical pH-adjusting reagents. Isotherm modeling confirmed a homogeneous monolayer physical adsorption process (Langmuir $R^2 = 0.99$; Dubinin-Radushkevich E < 8 kJ/mol) with a maximum adsorption capacity ($q_m = 12.13$ mg/g) more than double that of clay (5.00 mg/g).

Crucially, the ISO-compliant comparative Life Cycle Assessment (LCA) (ReCiPe 2008 Midpoint and Endpoint) confirmed the decisive environmental superiority of unfunctionalized RCD over natural clay. By avoiding energy-intensive clay mining and thermal activation while diverting construction waste from landfills, RCD drastically reduces climate change, fossil depletion, and human toxicity impacts. Sensitivity analyses across Hierarchist, Egalitarian, and Individualist perspectives consistently demonstrated substantially lower total damage scores for RCD compared to natural clay. Ultimately, this work proves that RCD is not merely a low-cost adsorbent but a viable, eco-efficient solution that bridges heavy metal remediation with sustainable resource management.

Declaration of Competing Interest: The authors declare that they have no known competing financial interests or personal relationships that could have appeared to influence the work reported in this article. In addition, no permission is required for the material used in this study.

Data availability: Data will be made available on request.

Funding Declaration: No funding was received for conducting this study.

Institutional Review Board Statement: Not applicable.

Ethics statement: The manuscript doesn't have any research that includes studies on human subjects, human data or tissue, or animals.

Declaration of AI use: The authors declare the use of generative artificial intelligence (AI) and AI-assisted technologies in the preparation of this manuscript. Specifically, Gemini was used to draw the graphical abstract of the article. The AI tool was not used for data analysis, interpretation of results, or drawing scientific conclusions. All content has been reviewed and verified by the authors to ensure accuracy and integrity.

Author contribution:

Radia Maachou, Hiba Ferhat, Abdelouahab Lefkir, Hakim Baloul, Abdelghani Bouchama, and **Yazid Chetbani:** Conceptualization, Data curation, Methodology, Formal analysis, Investigation, Visualization, Writing—original draft, and Validation; **Mostefa Hani, Nadjib Mebirouk, Ahmed Belaadi**, and **Herbert Mukalazi**: Conceptualization, Writing—review & editing, and Validation.

References

[1] W. Lu, J. Lou, C. Webster, F. Xue, Z. Bao, and B. Chi, "Estimating construction waste generation in the Greater Bay Area, China using machine learning," *Waste Manag.*, vol. 134, pp. 78–88, 2021.

[2] C.-S. Poon, X. C. Qiao, and D. Chan, "The cause and influence of self-cementing properties of fine recycled concrete aggregates on the properties of unbound sub-base," *Waste Manag.*, vol. 26, no. 10, pp. 1166–1172, 2006.

[3] C.-S. Poon and D. Chan, "The use of recycled aggregate in concrete in Hong Kong," *Resour. Conserv. Recycl.*, vol. 50, no. 3, pp. 293–305, 2007.

[4] H. Yang, J. Xia, J. R. Thompson, and R. J. Flower, "Urban construction and demolition waste and landfill failure in Shenzhen, China," *Waste Manag.*, vol. 63, pp. 393–396, 2017.

[5] M. Bensmail, R. Zaitri, M. Hani, Y. Chetbani, D. Benamara, and A. Laouissi, "Analyzing the effects of recycled aggregates on the workability and mechanical characteristics of concrete through mixture design and optimization techniques," *World J. Eng.*, vol. 23, no. 3, pp. 599–614, 2026.

[6] C. Belebchouche *et al.*, "Modeling of recycled coarse aggregates concrete characteristics via hybrid improved Grey Wolf Optimizer deep neural network and multi-objective Grey Wolf Optimization," *Results Eng.*, p. 108512, 2025.

[7] T. E. Oladimeji, M. Oyedemi, M. E. Emetere, O. Agboola, J. B. Adeoye, and O. A. Odunlami, "Review on the impact of heavy metals from industrial wastewater effluent and removal technologies," *Heliyon*, vol. 10, no. 23, 2024.

[8] N. A. A. Qasem, R. H. Mohammed, and D. U. Lawal, "Removal of heavy metal ions from wastewater: a comprehensive and critical review," *Npj Clean Water*, vol. 4, no. 1, p. 36, 2021.

[9] A. Gafoor, S. Kumar, S. Begum, and Z. Rahman, "Elimination of nickel (II) ions using various natural/modified clay minerals: A review," *Mater. Today Proc.*, vol. 37, pp. 2033–2040, 2021.

[10] N. P. Raval, P. U. Shah, and N. K. Shah, "Adsorptive removal of nickel (II) ions from aqueous environment: A review," *J. Environ. Manage.*, vol. 179, pp. 1–20, 2016.

[11] J. Briffa, E. Sinagra, and R. Blundell, "Heavy metal pollution in the environment and their toxicological effects on humans," *Heliyon*, vol. 6, no. 9, 2020.

[12] A. Alouache, A. Selatnia, H. E. Sayah, M. Khodja, S. Moussous, and N. Daoud, "Biosorption of hexavalent chromium and Congo red dye onto Pleurotus mutilus biomass in aqueous solutions," *Int. J. Environ. Sci. Technol.*, vol. 19, no. 4, pp. 2477–2492, 2022, doi: https://doi.org/10.1007/s13762-021-03313-2.

[13] H. Es-Sahbany *et al.*, "Removal of heavy metals (nickel) contained in wastewater-models by the adsorption technique on natural clay," *Mater. Today Proc.*, vol. 13, pp. 866–875, 2019.

[14] F. M. Azizi, "Utilisation d'un matériau argileux: traitement, caractérisation et application pour la dépollution des effluents inorganiques (métaux lourds) contenus dans les," 2018. [Online]. Available: https://repository.usthb.dz/bitstream/handle/123456789/7775/TH9128.pdf?sequence=3&isAllowed=y

[15] H. Ferhat *et al.*, "Innovative adsorption of lead and copper using recycled concrete in aqueous solutions," *Int. J. Chem. React. Eng.*, 2025, doi: doi:10.1515/ijcre-2025-0143.

[16] S. Kaza, L. Yao, P. Bhada-Tata, and F. Van Woerden, *What a waste 2.0: a global snapshot of*

solid waste management to 2050. World Bank Publications, 2018.

[17] N. Zhang, A. K. Konyalıoğlu, H. Duan, H. Feng, and H. Li, "The impact of innovative technologies in construction activities on concrete debris recycling in China: a system dynamics-based analysis," *Environ. Dev. Sustain.*, vol. 26, no. 6, pp. 14039–14064, 2023.

[18] A. Gallego-Schmid, H.-M. Chen, M. Sharmina, and J. M. F. Mendoza, "Links between circular economy and climate change mitigation in the built environment," *J. Clean. Prod.*, vol. 260, p. 121115, 2020.

[19] D. Hoornweg and P. Bhada-Tata, *What a waste: a global review of solid waste management*, vol. 15. World Bank Washington, DC, 2012.

[20] S. Nanda and F. Berruti, "Municipal solid waste management and landfilling technologies: a review," *Environ. Chem. Lett.*, vol. 19, no. 2, pp. 1433–1456, 2021.

[21] I. Messaoudene *et al.*, "Assessment of the role of blast furnace slag in optimising the physico-mechanical properties of compressed earth blocks stabilised with cement and lime," *Eur. J. Environ. Civ. Eng.*, vol. 29, no. 14, pp. 2956–2979, 2025.

[22] M. Hani and B. Evirgen, "Uncoupled thermo-hydro-mechanical modeling of a pykrete diaphragm wall for an alternative artificial ground freezing application," *Comput. Geotech.*, vol. 169, p. 106243, 2024.

[23] M. Hani and B. Evirgen, "A frozen soil sampling technique for granular soils and thermal modeling," *Bull. Eng. Geol. Environ.*, vol. 82, no. 9, p. 354, 2023.

[24] M. Hani and B. Evirgen, "The mechanical and microstructural properties of artificially frozen Sawdust–Ice mixture (PykRetE) and its usability as a retaining structure," *Int. J. Civ. Eng.*, vol. 21, no. 1, pp. 119–134, 2023.

[25] F. Cheriet, M. Hani, H. A. E. Ladjal, and B. Ben aziz, "A numerical simulation of slope stability with nailing and shotcreting techniques on natural ground," *Model. Earth Syst. Environ.*, vol. 10, no. 4, pp. 5399–5407, 2024.

[26] M. Sahraoui *et al.*, "AI-Driven predicting and optimizing lignocellulosic sisal fiber-reinforced lightweight foamed concrete: A machine learning and metaheuristic approach for sustainable construction," *Results Eng.*, vol. 26, p. 105561, 2025.

[27] Y. Kellouche *et al.*, "Prediction and optimization of the compressive strength of marble powder-based concrete using AI techniques: Machine learning and metaheuristic approaches," *Model. Earth Syst. Environ.*, vol. 11, no. 6, p. 413, 2025.

[28] H. Ben Salah and M. Hani, "An investigation of the effect of high temperature on the strength compression and ultrasonic pulse velocity of self-compacting concrete," 2024.

[29] L. Lemire, S. Reyes, Y. Durocher, R. Voyer, O. Henry, and P. L. Pham, "Scale-up of a monoclonal antibody CHO fed-batch production in stirred tank bioreactors: Effect of hydrodynamic conditions and feeding regimen," *Biotechnol. Prog.*, vol. 42, no. 1, p. e70073, 2026.

[30] ISO 14040, "Environmental assessment - Life cycle assessment - Principles and framework," *Int. Stand. Organ.*, vol. 1997, pp. 1–20, 2006.

[31] Y. Li, X. Luo, X. Huang, D. Wang, and W. Zhang, "Life cycle assessment of a municipal wastewater treatment plant: a case study in Suzhou, China," *J. Clean. Prod.*, vol. 57, pp. 221–227, 2013.

[32] A. S. Bello, N. Zouari, D. A. Da'ana, J. N. Hahladakis, and M. A. Al-Ghouti, "An overview of brine management: Emerging desalination technologies, life cycle assessment, and metal

recovery methodologies," *J. Environ. Manage.*, vol. 288, p. 112358, 2021.

[33] Y. Zhang, K. Yuan, L. Magagnin, X. Wu, Z. Jiang, and W. Wang, "Selective adsorption of Pb (II) and Cu (II) on mercapto-functionalized aerogels: experiments, DFT studies and LCA analysis," *J. Clean. Prod.*, vol. 393, p. 136126, 2023, doi: https://doi.org/10.1016/j.jclepro.2023.136126.

[34] I. Marouani *et al.*, "Integration of renewable-energy-based green hydrogen into the energy future," *Processes*, vol. 11, no. 9, p. 2685, 2023.

[35] E. Vahidi, J. Navarro, and F. Zhao, "An initial life cycle assessment of rare earth oxides production from ion-adsorption clays," *Resour. Conserv. Recycl.*, vol. 113, pp. 1–11, 2016.

[36] I. ISO, "14040," *Environ. Manag. cycle assessment—principles Framew.*, vol. 578, pp. 235–248, 2006.

[37] G. Wernet, C. Bauer, B. Steubing, J. Reinhard, E. Moreno-Ruiz, and B. Weidema, "The ecoinvent database version 3 (part I): overview and methodology," *Int. J. life cycle Assess.*, vol. 21, no. 9, pp. 1218–1230, 2016.

[38] M. Z. Hauschild, R. K. Rosenbaum, and S. I. Olsen, "Life Cycle Assessment: Theory and Practice," *Life Cycle Assess. Theory Pract.*, pp. 1–1216, 2017, doi: 10.1007/978-3-319-56475-3.

[39] P. Wijeyawardana, D. Law, C. Gunasekara, N. Nanayakkara, A. Karunarathna, and B. K. Pramanik, "Assessing the life cycle and economic impact of cement-modified biochar compared to conventional adsorbents for heavy metal removal in stormwater," *Process Saf. Environ. Prot.*, vol. 192, pp. 244–256, 2024, doi: https://doi.org/10.1016/j.psep.2024.10.050.

[40] M. A. J. Huijbregts *et al.*, "ReCiPe2016: a harmonised life cycle impact assessment method at midpoint and endpoint level," *Int. J. life cycle Assess.*, vol. 22, no. 2, pp. 138–147, 2017, doi: https://doi.org/10.1007/s11367-016-1246-y.

[41] T. Zhang *et al.*, "Removal of heavy metals and dyes by clay-based adsorbents: From natural clays to 1D and 2D nano-composites," *Chem. Eng. J.*, vol. 420, p. 127574, 2021.

[42] M. K. Uddin, "A review on the adsorption of heavy metals by clay minerals, with special focus on the past decade," *Chem. Eng. J.*, vol. 308, pp. 438–462, 2017, doi: 10.1016/j.cej.2016.09.029.

[43] R. Mukhopadhyay *et al.*, "Clay–polymer nanocomposites: Progress and challenges for use in sustainable water treatment," *J. Hazard. Mater.*, vol. 383, p. 121125, 2020.

[44] G. Lo Dico, L. Lisuzzo, V. Carcelén, G. Cavallaro, and M. Haranczyk, "Thermogravimetric Analysis of Moisture in Natural and Thermally Treated Clay Materials.," *Mater. (Basel, Switzerland)*, vol. 17, no. 10, May 2024, doi: 10.3390/ma17102231.

[45] A. Benamor, C. Kadiri, Y. Derouiche, and A. Ouali, "Investigating the thermal behavior and dehydroxylation kinetics of bentonite: isothermal and non-isothermal study.," *High Temp. Press.*, vol. 53, no. 4, 2024.

[46] M. Aliu, M. Kelmendi, L. Pula-Beqiri, M. Sadiku, and S. Kadriu, "RESEARCH OF KARAÇEVA BENTONITE IN NATURAL STATE AND AFTER TREATMENT," *Rasayan J. Chem.*, vol. 11, no. 2, 2018.

[47] M. T. Zöllner, P. Dariz, J. Riedel, and T. Schmid, "Dolomite and Mg Calcite as Mineral Thermometers in Mortar Binders. A High Resolution Raman Spectroscopic Study," *J. Raman Spectrosc.*, vol. 56, no. 10, pp. 1059–1071, Oct. 2025, doi: https://doi.org/10.1002/jrs.6810.

[48] F. Y. Al-saffar, L. S. Wong, and S. C. Paul, "An Elucidative Review of the Nanomaterial Effect on the Durability and Calcium-Silicate-Hydrate (C-S-H) Gel Development of Concrete," 2023.

doi: 10.3390/gels9080613.

[49] L. Hanžič *et al.*, "Experimental Carbonation Study for a Durability Assessment of Novel Cementitious Materials," 2021. doi: 10.3390/ma14216253.

[50] D. Barbir, P. Dabić, M. Jakić, and I. Weber, "Evaluating the Heat of Hydration, Conductivity, and Microstructural Properties of Cement Composites with Recycled Concrete Powder," 2025. doi: 10.3390/buildings15152613.

[51] T. Papalas, A. N. Antzaras, and A. A. Lemonidou, "Integrated CO2 Capture and Utilization by Combining Calcium Looping with CH4 Reforming Processes: A Thermodynamic and Exergetic Approach," *Energy & Fuels*, vol. 38, no. 13, pp. 11966–11979, Jul. 2024, doi: 10.1021/acs.energyfuels.4c01462.

[52] E. J. C. Cea *et al.*, "Combined Effect of Multi-Walled Carbon Nanotubes and Silica Fume on Mechanical, Physicochemical, and Thermal Properties of Concrete Composites," 2025. doi: 10.3390/buildings15071087.

[53] A. Gorączko and S. Topoliński, "Particle size distribution of natural clayey soils: A discussion on the use of laser diffraction analysis (LDA)," *Geosciences*, vol. 10, no. 2, p. 55, 2020.

[54] C. Polakowski, M. Ryżak, A. Sochan, M. Beczek, R. Mazur, and A. Bieganowski, "Particle size distribution of various soil materials measured by laser diffraction—the problem of reproducibility," *Minerals*, vol. 11, no. 5, p. 465, 2021.

[55] J. Laible *et al.*, "Comparison of grain size distribution measurements of sand-silt mixtures using laser diffraction systems," *J. Soils Sediments*, vol. 23, no. 5, pp. 2310–2325, 2023, doi: 10.1007/s11368-023-03470-6.

[56] S. Wang *et al.*, "Experimental Research on the Performance of Recycled Waste Concrete Powder (RWCP) on Concrete.," *Mater. (Basel, Switzerland)*, vol. 17, no. 21, Oct. 2024, doi: 10.3390/ma17215319.

[57] F. Ippolito, G. Hübner, T. Claypole, and P. Gane, "Impact of bimodal particle size distribution ratio of functional calcium carbonate filler on thermal and flowability properties of polyamide 12," *Appl. Sci.*, vol. 11, no. 2, p. 641, 2021.

[58] C. Knoeri, E. Sanyé-Mengual, and H.-J. Althaus, "Comparative LCA of recycled and conventional concrete for structural applications," *Int. J. life cycle Assess.*, vol. 18, no. 5, pp. 909–918, 2013.